Astronomie et astrophysique pour physiciens CUSO 2012

Instruments and observational techniques – Interferometry

F. Pepe
Observatoire de l'Université Genève
F. Courbin and P. Jablonka, EPFL

Credits:

High angular resolution imaging and interferometry: An introduction to Fourier Optics and Coherence

D. Ségransan
Observatoire de Genève

Credit on the Content and slides :

- J.-M. Mariotti, lecture on Fourier Optics, Diffraction limited imaging with the VLT, Gargèse 1989
- C.D. Haniff, lecture on Inteferometry, *Observation and data reduction with the VLTI, Goutelas, 2006*

References :

- Born and Wolf, Principle of Optics
- Goodman, Statistical Optics

Preamble :

A brief history of long baseline interferometry and high angular resolution imaging

Fizeau interferometer at the Hooker telescope, Mt Wilson
Michelson, 1920

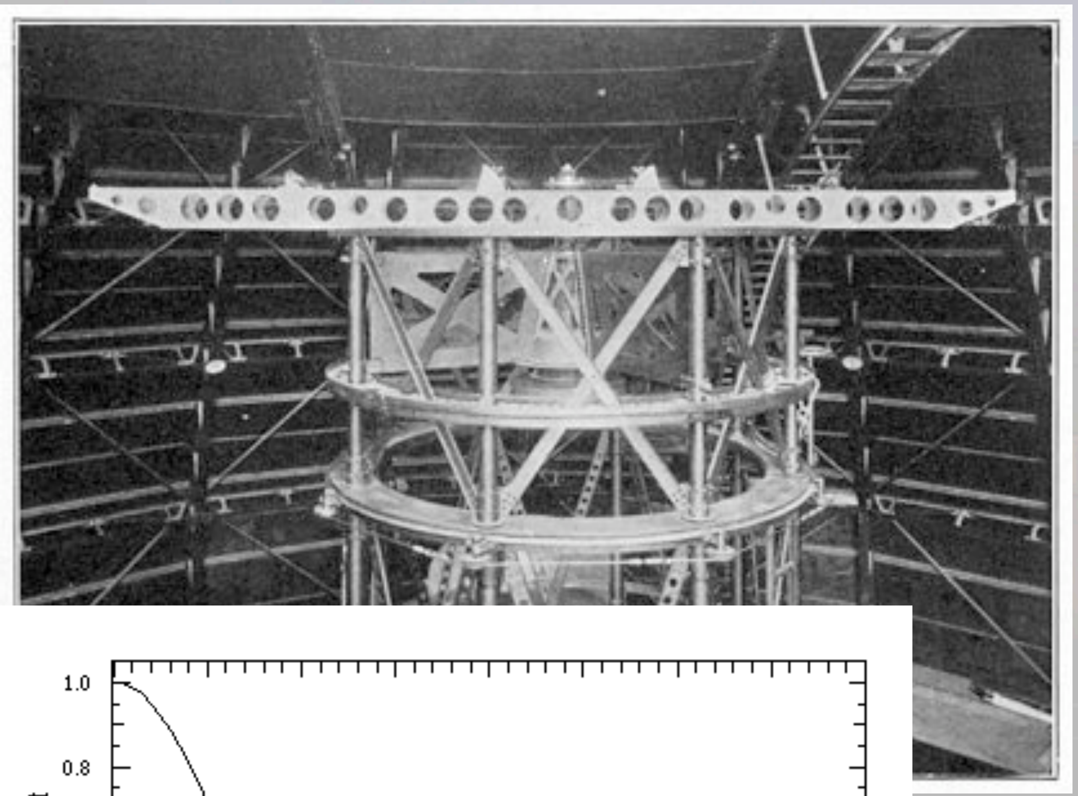

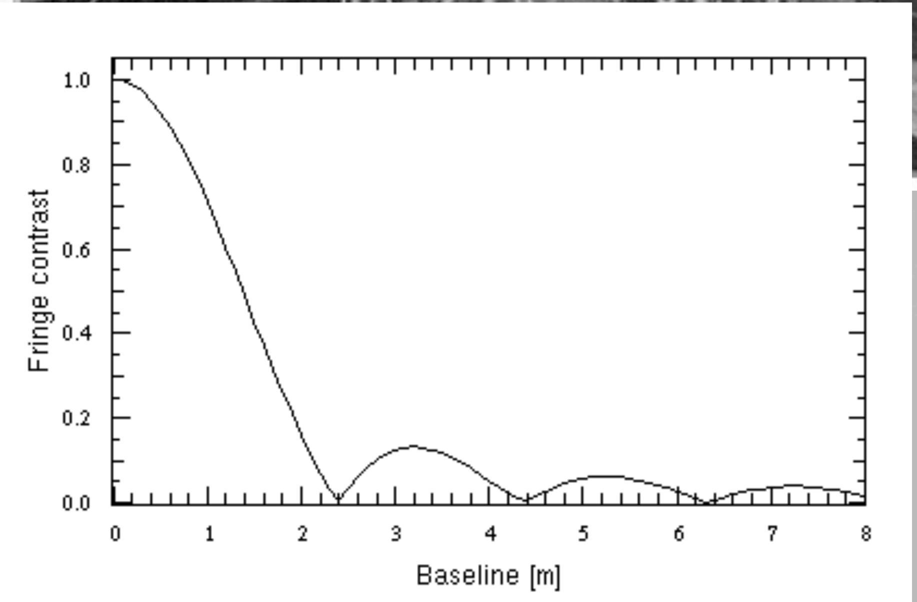

Facts :
Telescope : 2.54 m
Baseline : 6 m
4 movable mirrors: 10 cm

Wavelength : visible
Detector : the eyes !!!

Seeing : 1-2 arcsec
$\theta_{max}=\lambda/B=$ 19 mas

Stellar diameter of
Betelgeuse : 47 mas

Recent obs : 58 mas

Interferometry after the 1920's

Michelson's stellar interferometer remained a one shot experiment. Optical interferometry was too demanding for the technology of the 1920's. One will have to wait until A. Labeyrie's I2T experiment in the 1970's to hear about long baseline interferometry at optical wavelength.

However, the story was different at radio wavelength. To compensate for the lack of angular resolution of single dish antennas (1.14deg or 4000 arcsec!), radio interferometry was first used in 1946. It completely dominated the field for the next 30-40 years.

Very Large Array, Socorro, NM, 1980

Radio wavelength : cm (2-20)

27 Antennas

Y-shape baselines 21km

Special baseline : 36km

Angular resolution : 50mas – 1 arcsec

Nearby merging galaxy, NGC 4038

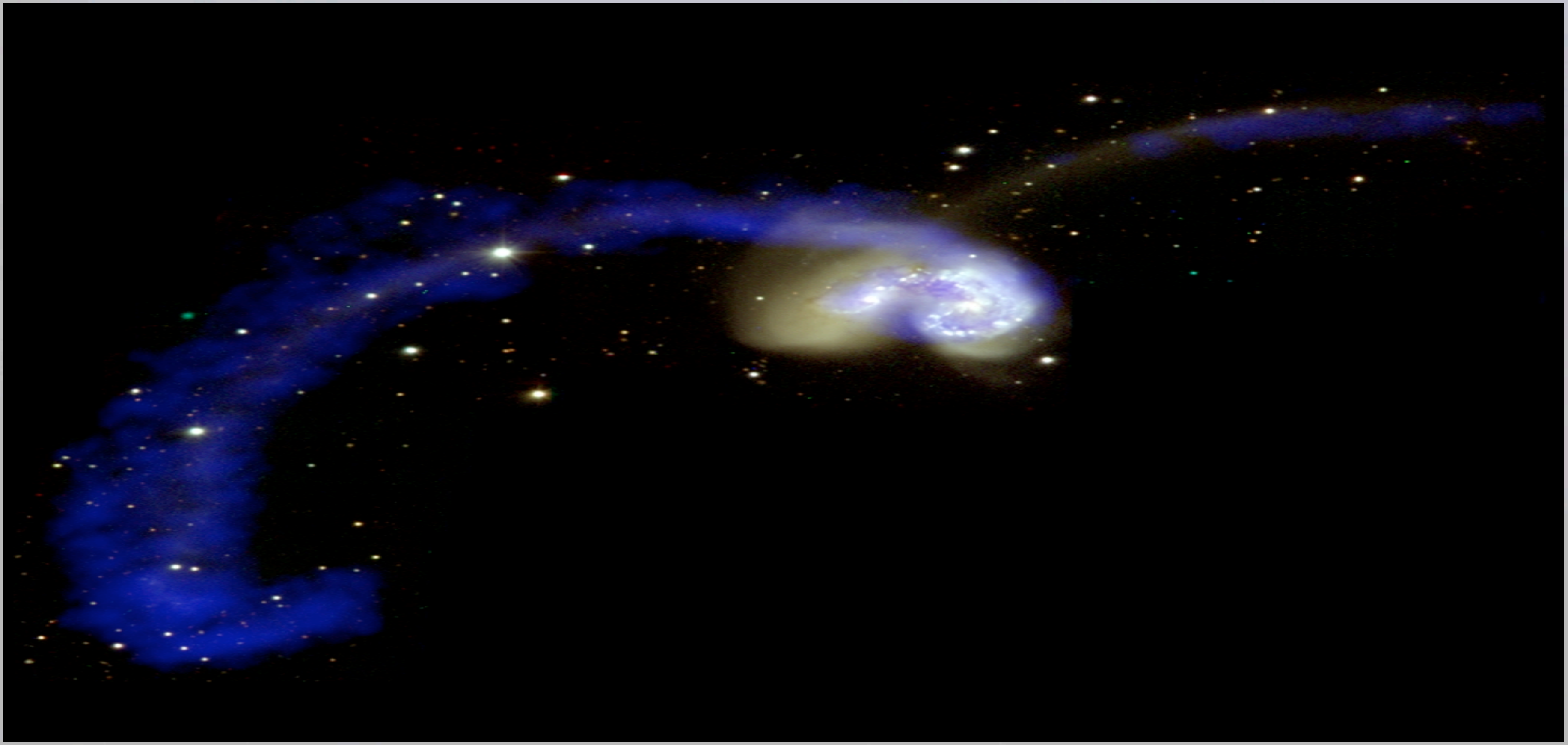

The image shows a true-color representation of the optical starlight, with the neutral atomic gas depicted in blue. This system is composed of two spiral galaxies which are in the process of slamming together, throwing off two long, narrow tidal streamers. The atomic hydrogen observations, obtained with the VLA, provide information on both the distribution of the gas (as shown), as well as its kinematics.

IRAM, Plateau de Bure, Hautes-Alpes, 1988

mm wavelengths : 1-3 mm
6 antennas
baselines up to 760m
Angular resolution : 270mas – 1 arcsec

Continuum emission in NGC1068, a bright, nearby (D=14Mpc) active galaxy

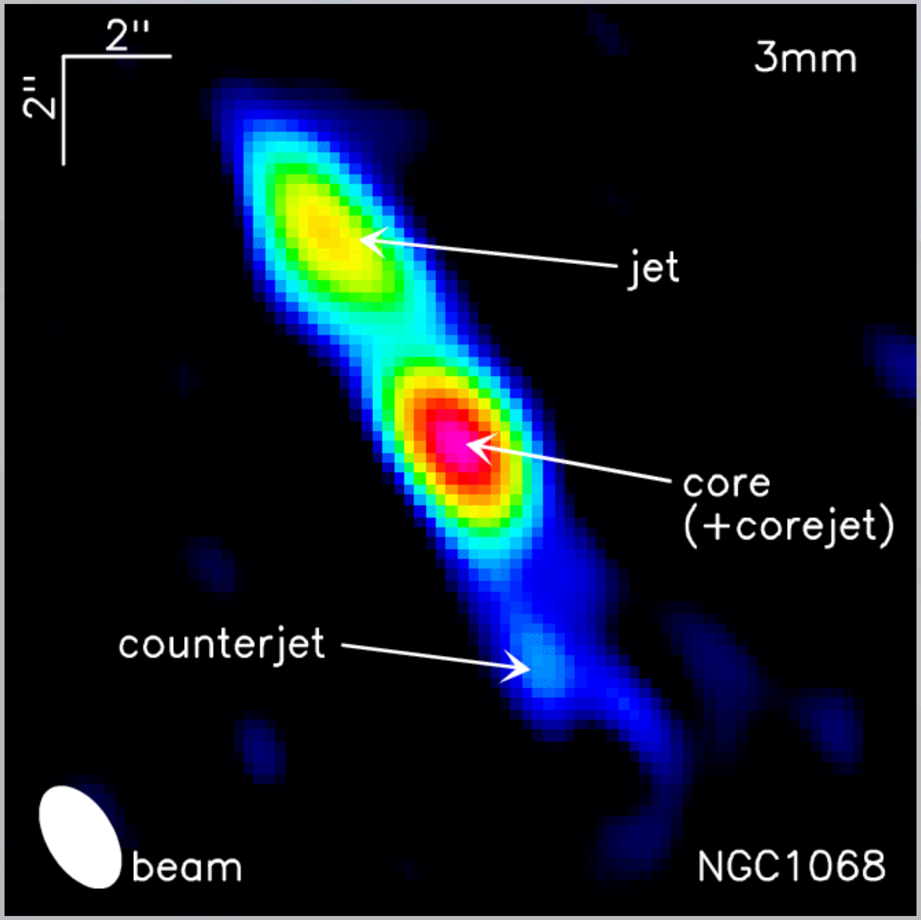

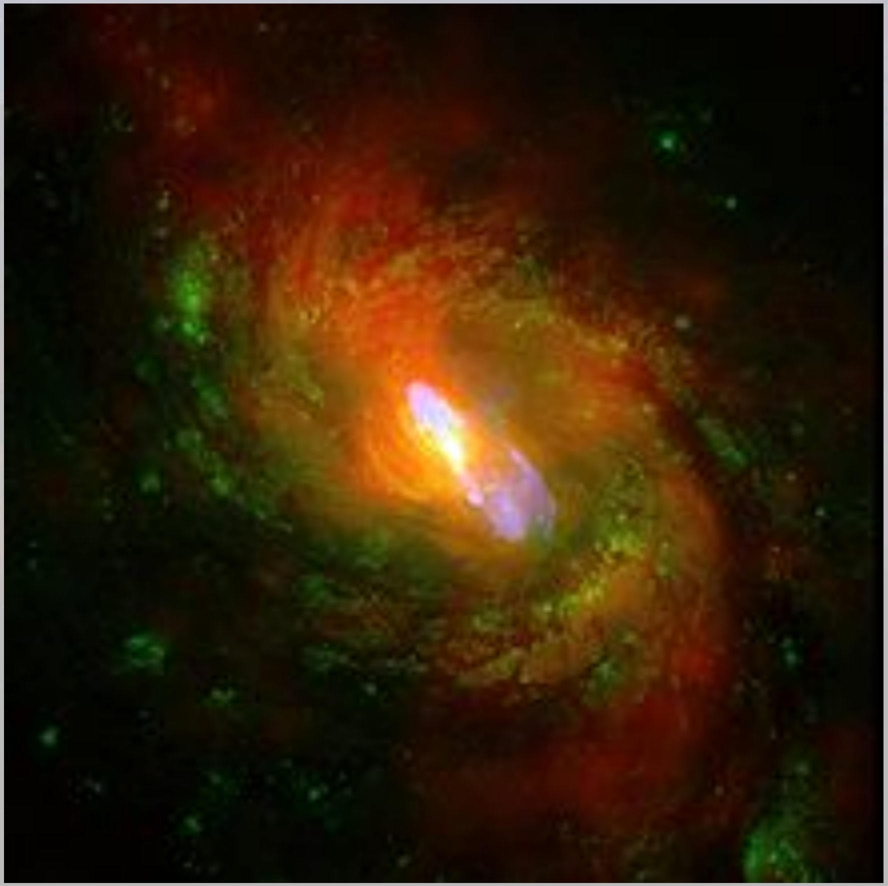

High angular resolution observations carried out at 3mm and 1mm with the IRAM. Three continuum peaks are detected in NGC1068, one centered on the core, one associated with the jet and a third one with the counter-jet.

CFHT-PUEO, Mauna Kea, 1997

wavelengths : 1.25-2.2 µm
Diameter : 3.6m
Angular resolution : 126mas in K

Observations of the Galactic Center

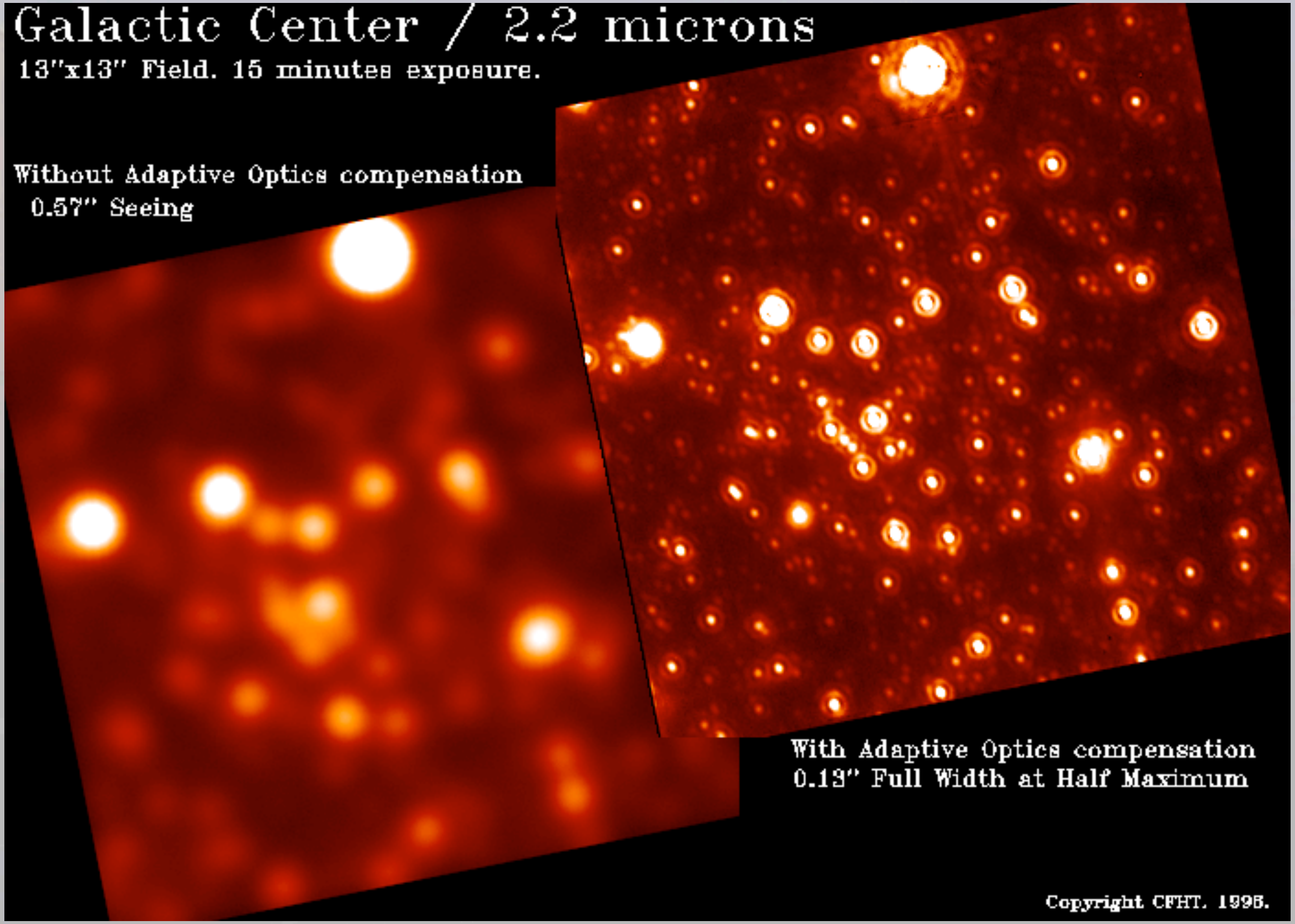

VLT-NACO, Paranal, 2002

wavelengths : 1.25-5 µm
Diameter : 8.2m
Angular resolution : 56mas in K

Observations of the Galactic Center

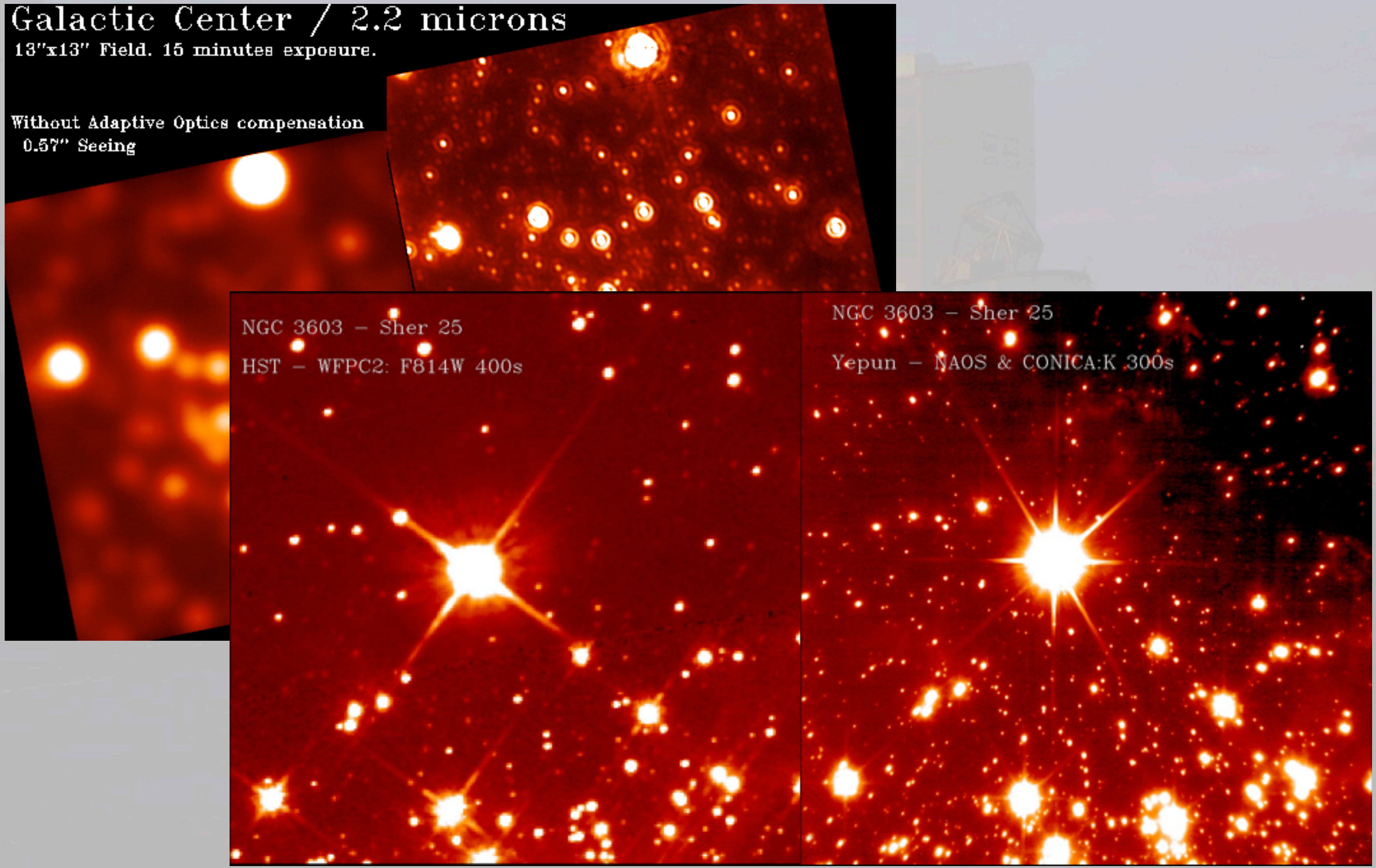

Bird' interacting galaxy system with NACO and HST

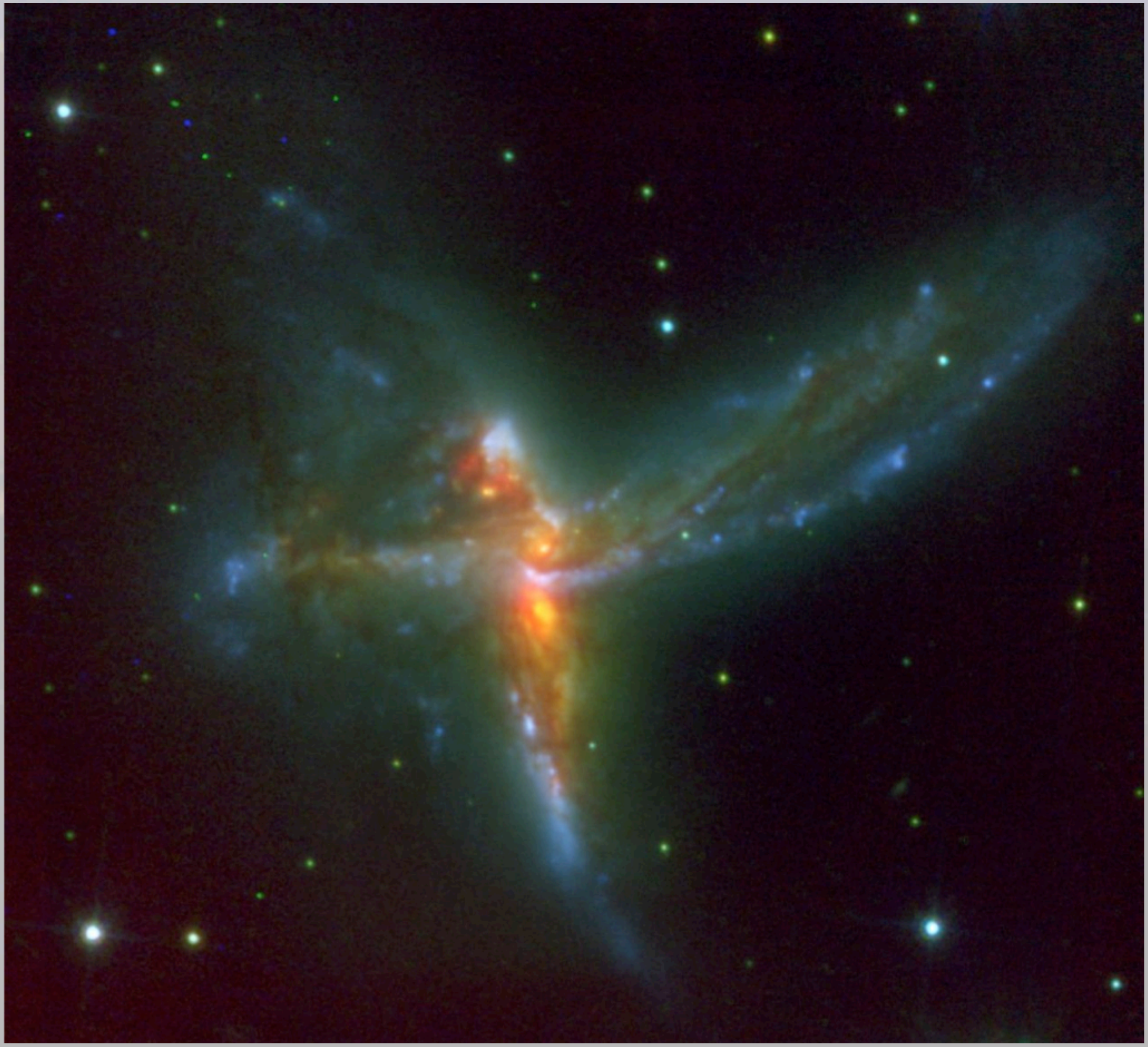

VLTI, Paranal, 2002

Near and mid IR

Recombine up to
4 8-meter-telescopes
4 1.8-meter-telescopes

Baselines up to 180m

Angular resolution :
2.5-25mas in K

Imaging with the VLTI

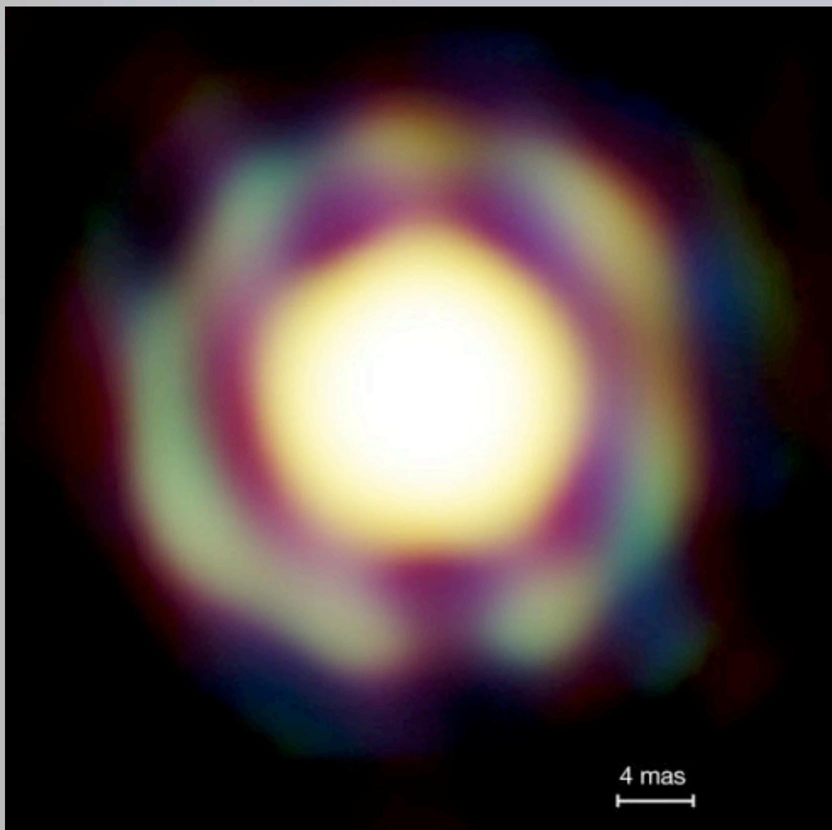

The Mira star T Leporis

The star is surrounded by a spherical shell of molecular material expelled from the star.

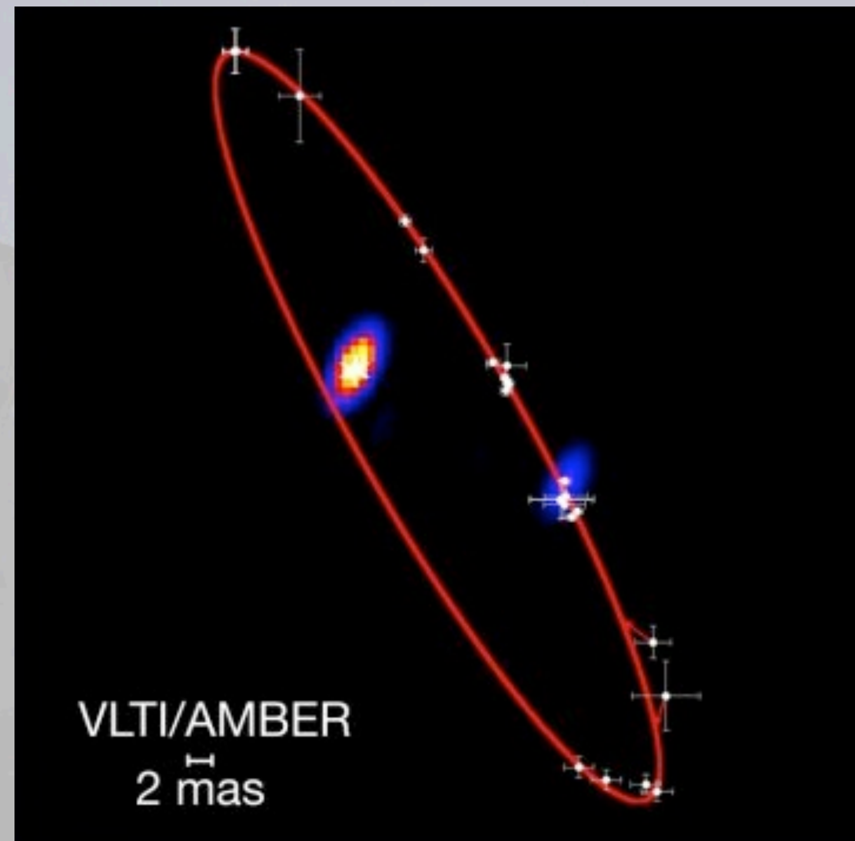

The orbit of Theta1 Orionis C

The total mass of the two stars (47 solar masses)

What do we observe?

- Consider a perfect telescope in space observing an unresolved point source:
  - This produces an Airy pattern with a characteristic width: $\theta = 1.22\lambda/D$ in its focal plane.
  - θ is the approximate angular width of the image, called the "angular resolution".
  - λ is the wavelength at which the observation is made.
  - D is the diameter of the telescope aperture, assumed circular here.

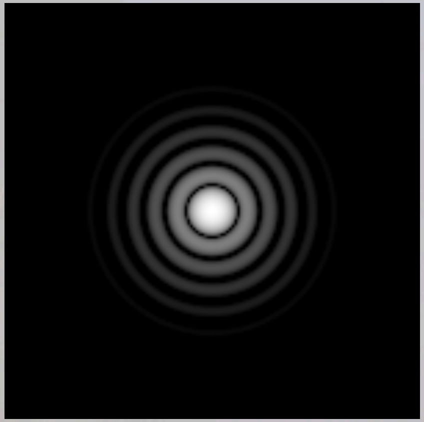

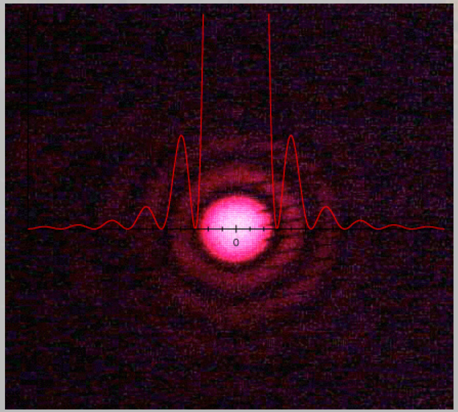

How does this impact imaging?

- Image formation (under incoherent & isoplanatic conditions):
  - Each point in the source produces a displaced Airy pattern. The superposition of these limits the detail visible in the final image.

- But what causes the Airy pattern?
  - **Interference** between parts of the wavefront that originate from different regions of the aperture.
  - In this case, the relative amplitude and phase of the field at each part of the aperture are what matter.

Remember: Image formation

(1) $$\check{u}(\vec{k}) = \frac{u_0}{2\pi} \int T(x,y) \cdot e^{+i(\vec{k}-\vec{k}_0)\vec{x}} \, dx \, dy$$

(2) $$I(\vec{k}) = \frac{|\check{u}(\vec{k})|^2}{2} = \frac{u_0^2}{8\pi^2} \cdot \left|\check{T}(\vec{k}-\vec{k}_0)\right|^2$$

Def.: $\mathrm{PSF} = |\check{T}(\vec{k})|^2$ = Point-Spread-Function

(3) $$I(\vec{k}) = \int A(\vec{k}') \cdot \mathrm{PSF}(\vec{k}-\vec{k}') \, dk'_x \, dk'_y$$

Where A(k) = intensity distribution of source

A two element interferometer - function

- Sampling of the radiation (from a distant point source).
- Transport to a common location.
- Compensation for the geometric delay.
- Combination of the beams.
- Detection of the resulting output.

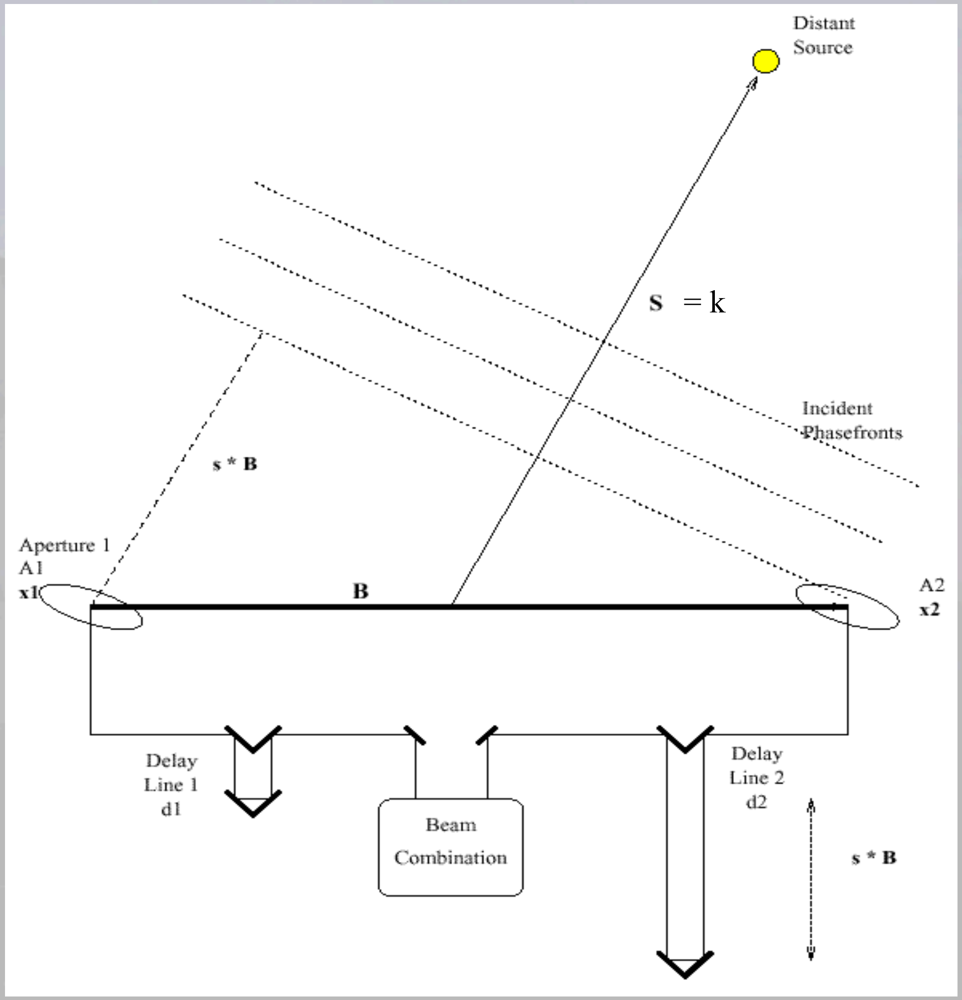

A two element interferometer - nomenclature

- Telescopes located at x_1, x_2.
- Baseline B = $(x_1 - x_2)$.
- Pointing direction towards source is S.
- Geometric delay is $\hat{s}.B$, where $\hat{s} = S/|S|$.
- Optical paths along two arms are d_1 and d_2.

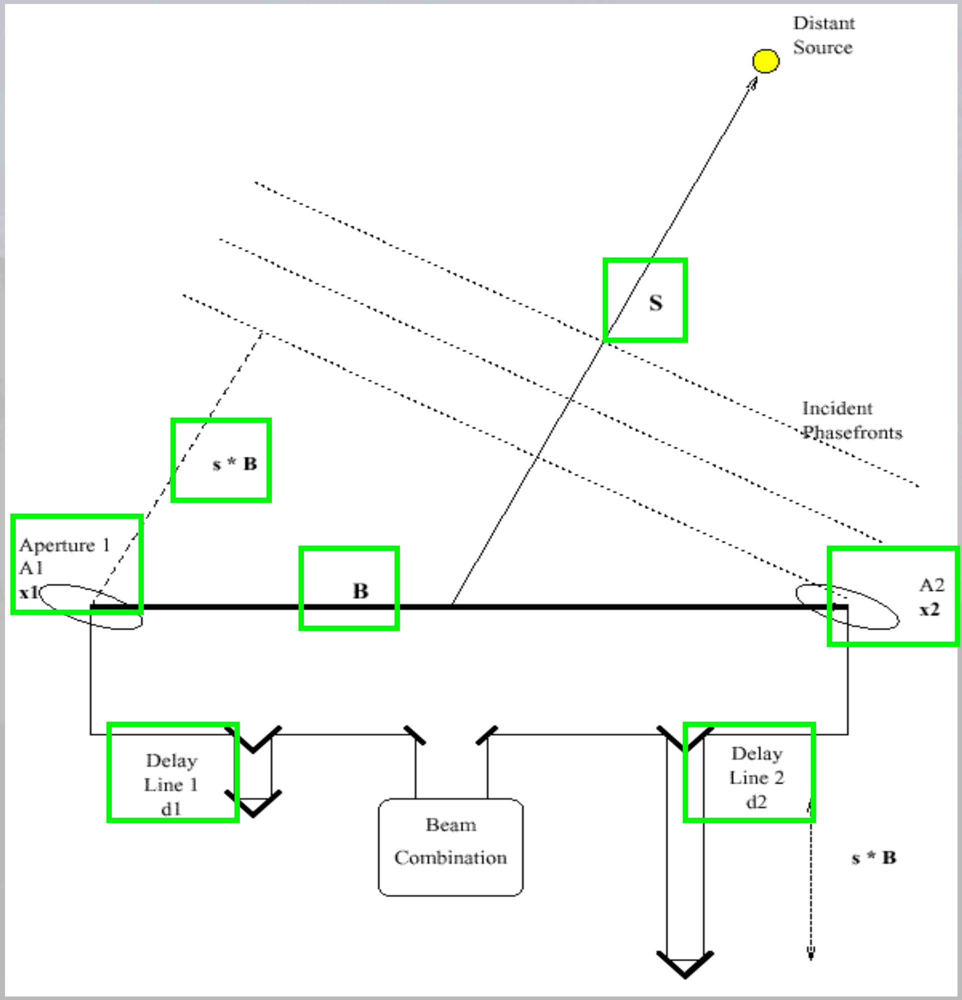

2-telescope interferometry

Interféromètre à deux télescopes :

$$T(\vec{x}_T) = T_{Tel}\left(\vec{x}_T - \frac{\vec{B}}{2}\right) + T_{Tel}\left(\vec{x}_T + \frac{\vec{B}}{2}\right)$$

$$\Rightarrow \check{u}_s'(\vec{k}) = u_0 \left[\check{T}_{Tel}(\vec{k}-\vec{k}_0)\, e^{-i(\vec{k}-\vec{k}_0)\frac{\vec{B}}{2}} + \check{T}_{Tel}(\vec{k}-\vec{k}_0) \cdot e^{+i(\vec{k}-\vec{k}_0)\frac{\vec{B}}{2}} \right]$$

$$= 2u_0\, \check{T}_{Tel}(\vec{k}-\vec{k}_0) \cdot \cos\left[(\vec{k}-\vec{k}_0)\cdot\frac{\vec{B}}{2}\right]$$

$$\Rightarrow PSF(\vec{k}) = \left| \frac{\check{u}_s'(\vec{k}-\vec{k}_0)}{2u_0} \right|^2 = PSF_{Tel}(\vec{k}-\vec{k}_0) \cdot \underbrace{\cos^2\left[(\vec{k}-\vec{k}_0)\cdot\frac{\vec{B}}{2}\right]}_{=:PSF_{INT}}$$

Image plane intensity distribution

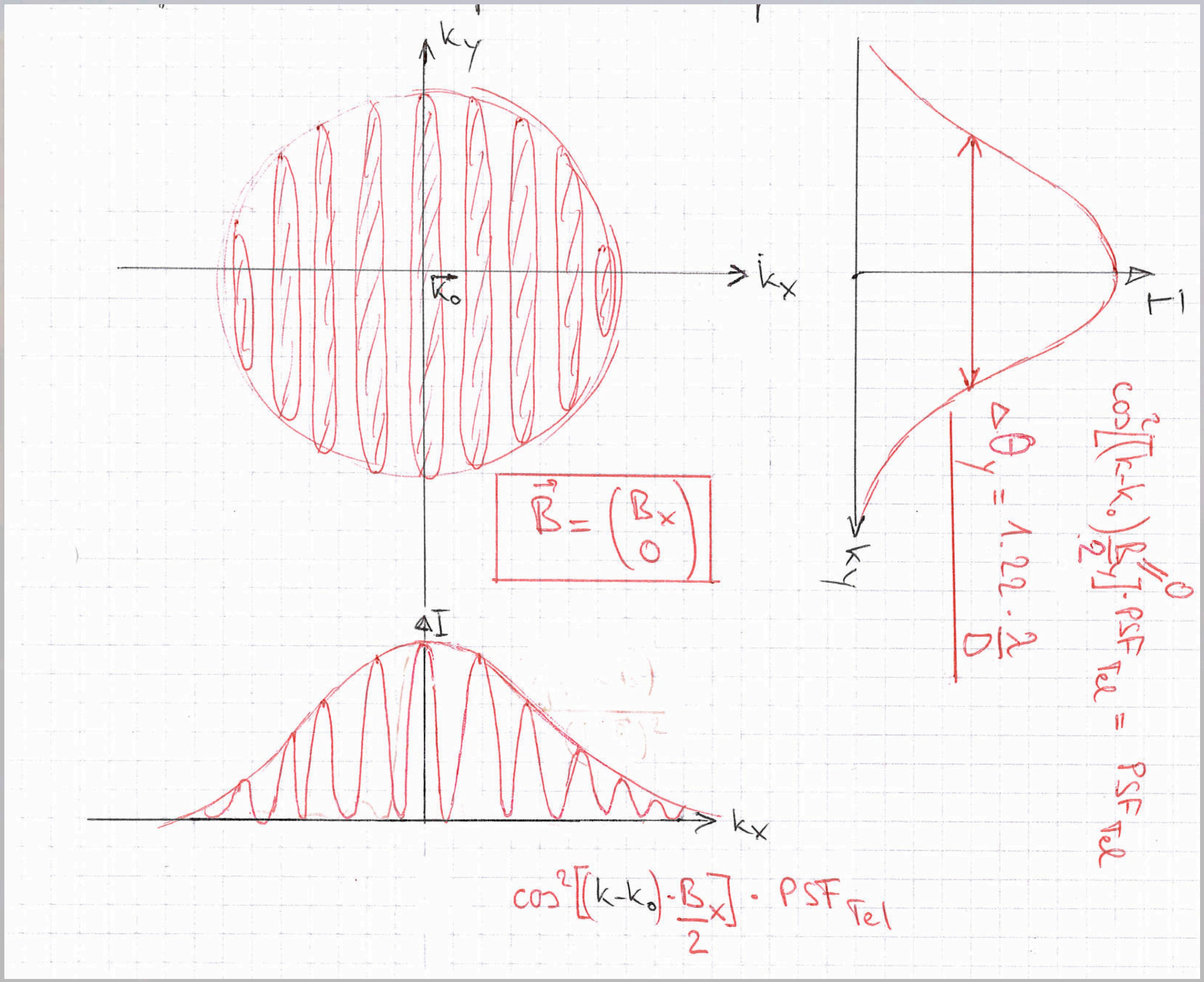

Image plane intensity distribution

- Resolution dans la direction k_y $\equiv$ Resolution du Telescope avec D

$$\Delta\theta_y = 1.22 \cdot \frac{\lambda}{D}$$

- Resolution dans la direction k_x :

Premier minimum pour $\Delta k \cdot \frac{B_x}{2} = \pi$

$$\Rightarrow \frac{2\pi}{\lambda} \cdot \Delta\theta_x \cdot \frac{B_x}{2} = \pi$$

$$\Rightarrow \Delta\theta_x = \frac{\lambda}{B_x}$$

$\Rightarrow$ Résolution en k_x est equivalente à télescope de diamètre B_x !

Illustration : a binary star

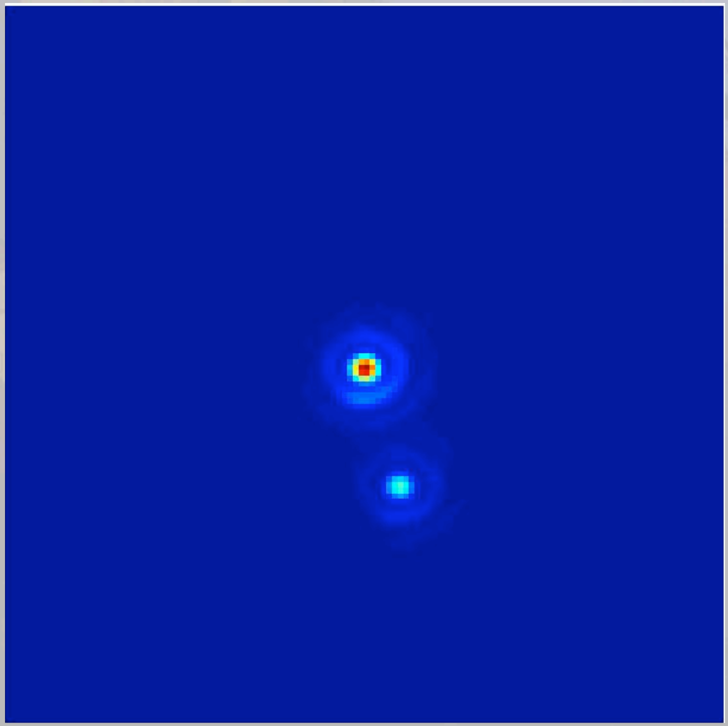

Single telescope with diameter D

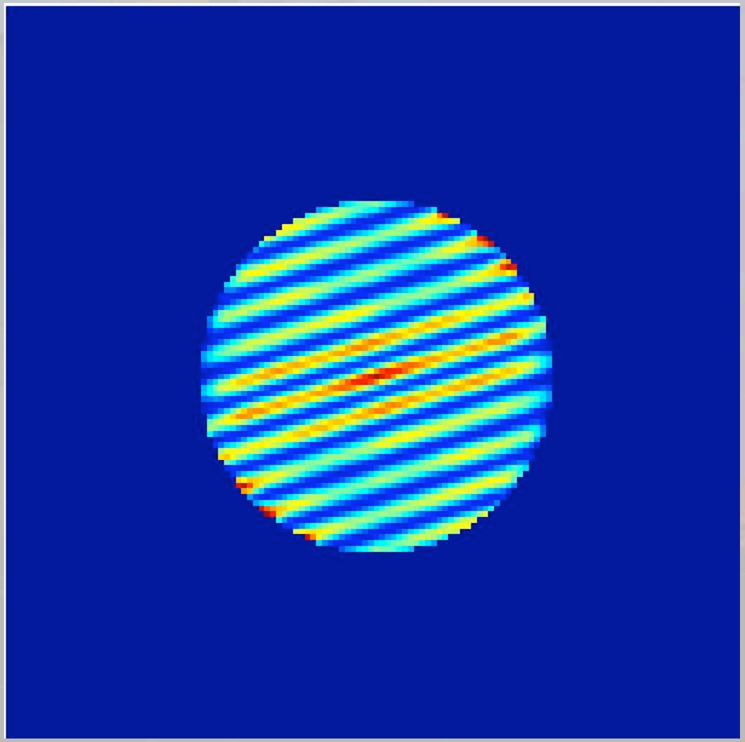

2 telescopes separated by D
And of diameter d << D

Extended source

$I(\vec{k})$ receives contributions from various sources $\vec{k}_s$ with intensity $A(\vec{k}_s)$.

$$I(\vec{k}) = \int_s I_s(\vec{k}) = \int_{k_s} A(\vec{k}_s) \cdot PSF_{Tel}(\vec{k}_s - \vec{k}) \cdot PSF_{int}(\vec{k}_s - \vec{k}) \, dk_s$$

$$=: A \otimes PSF_{Tot}(\vec{k})$$

Extended source

Let's simplify: PSF_{Tel} = slowly varying function ≈ 1

$$\Rightarrow I(\vec{k}) = \underbrace{\int A(\vec{k}_s)\, dk_s}_{I_s} + \int A(\vec{k}_s) \cdot \cos\left((\vec{k}_s - \vec{k}) \cdot \vec{B}\right) dk_s$$

$$= I_s + \mathrm{Re}\left| \int A(\vec{k}_s) \cdot e^{-i(\vec{k}_s - \vec{k}) \cdot \vec{B}}\, dk_s \right|$$

$$= I_s + \mathrm{Re}\left| e^{i\vec{k}\vec{B}} \cdot \underbrace{\int A(\vec{k}_s)\, e^{-i\vec{k}_s \vec{B}}\, dk_s}_{V = \text{visibility}} \right|$$

$$= I_s + \cos(\vec{k}\vec{B}) \cdot \mathrm{Re}\, V + \sin(\vec{k}\vec{B}) \cdot \mathrm{Im}\, V$$

Measurements of fringes

- From an interferometric point of view the key features of any interference fringe are its modulation and its location with respect to some reference point.

- In particular we can identify:
  - The fringe visibility:

$$V = \frac{[I_{max} - I_{min}]}{[I_{max} + I_{min}]}$$

  - The fringe phase:
    - The location of the white-light fringe as measured from some reference (radians).

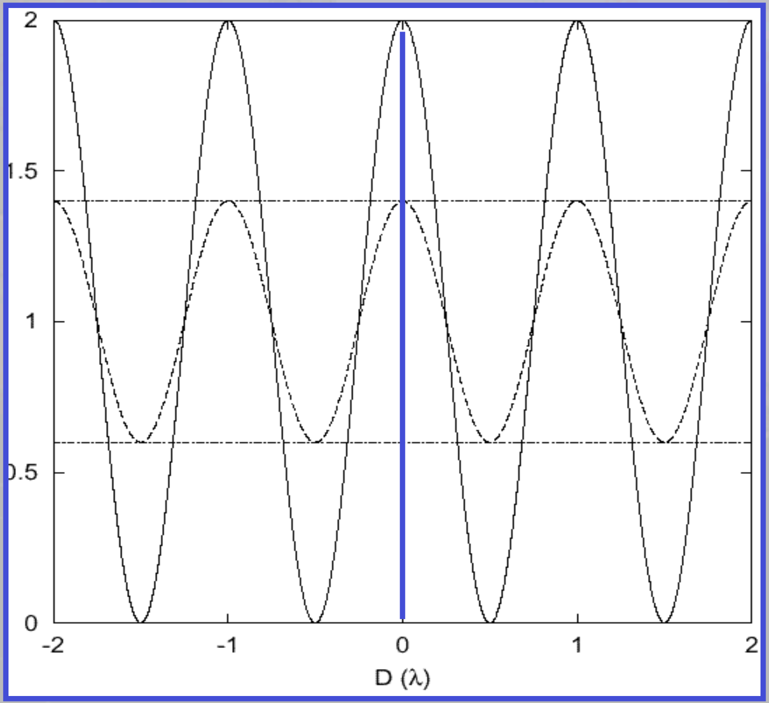

These measure the amplitude and phase of the complex coherence function, respectively.

The output of a 2-element interferometer (ii)

- The output varies co-sinusiodally with D.
- Adjacent fringe peaks are separated by
  $\Delta d_{1 \text{ or } 2} = \lambda$
  or
  $\Delta(\hat{s}.B) = \lambda$.

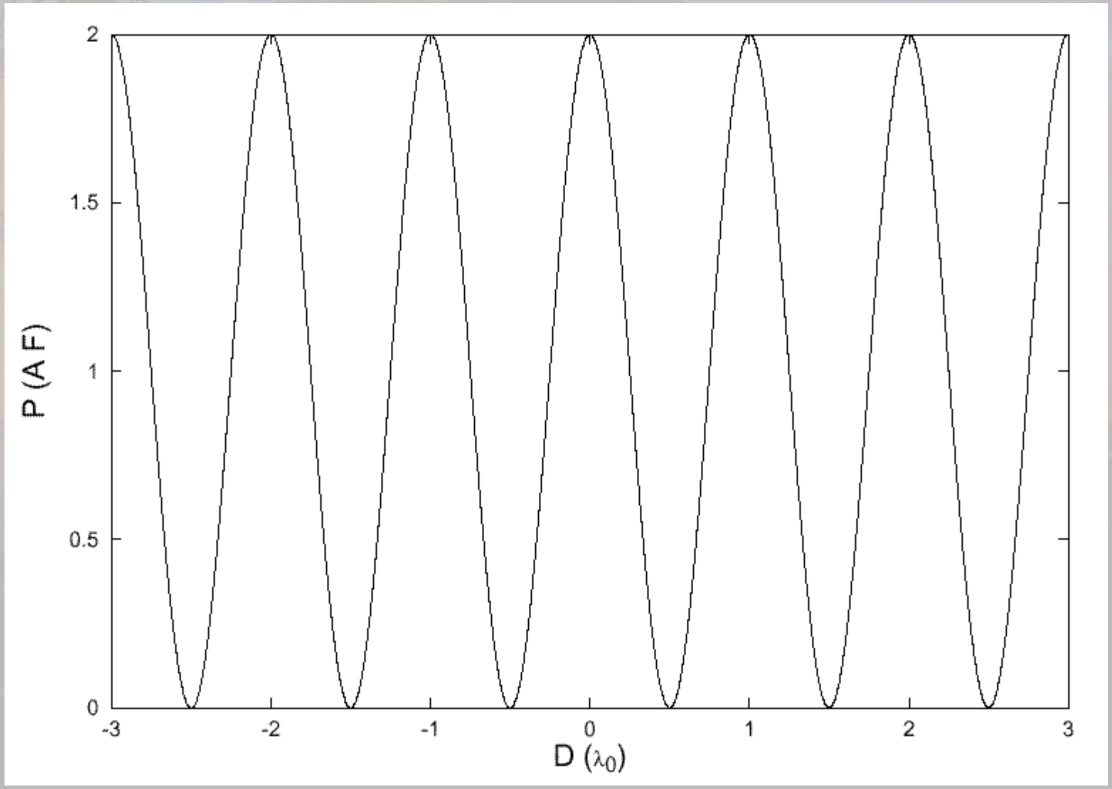

Heuristic operation of an interferometer

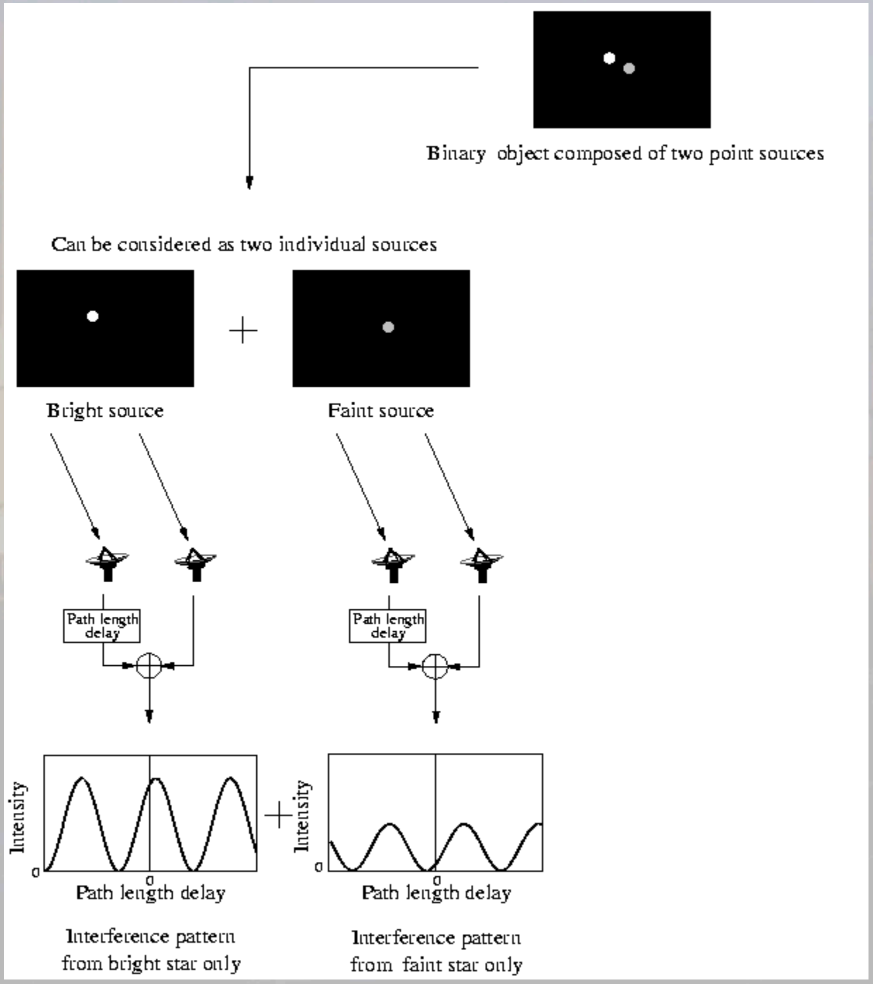

- Each unresolved element of the image produces its own fringe pattern.
- These have unit visibility and a phase that is associated with the location of the element in the sky.

Heuristic operation of an interferometer

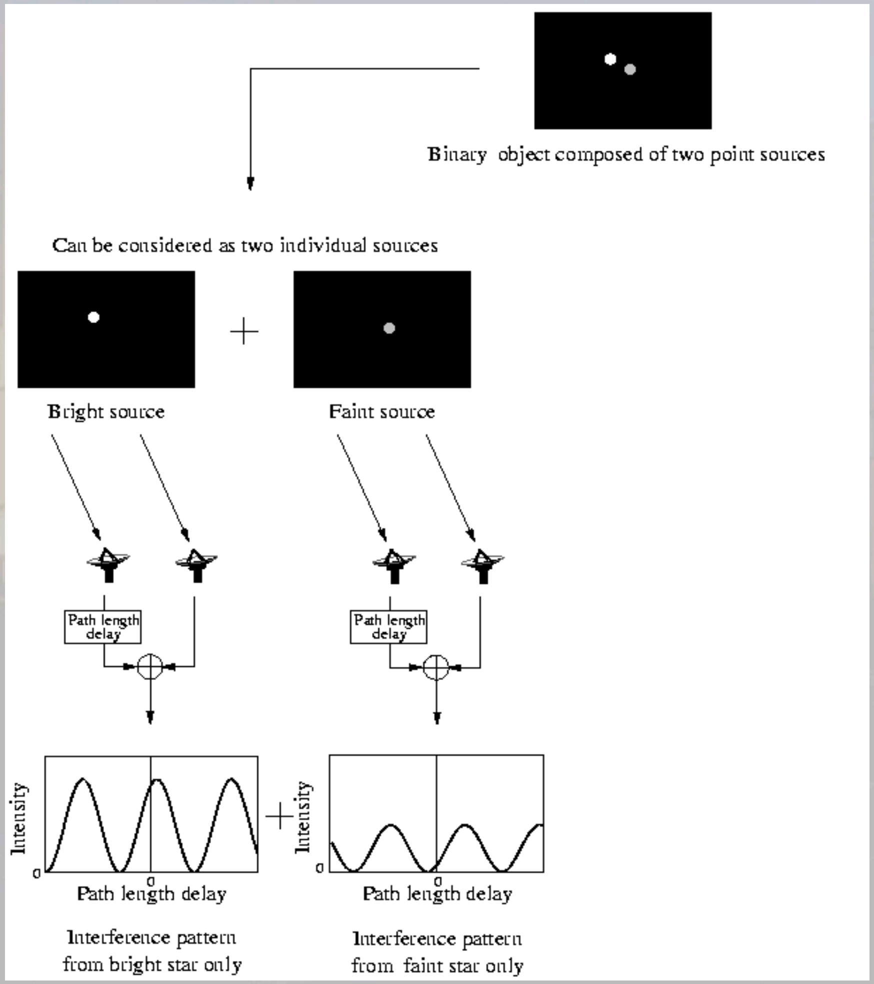

- The observed fringe pattern from a distributed source is just the intensity superposition of these individual fringe pattern.
- This relies upon the individual elements of the source being "spatially incoherent".

Heuristic operation of an interferometer

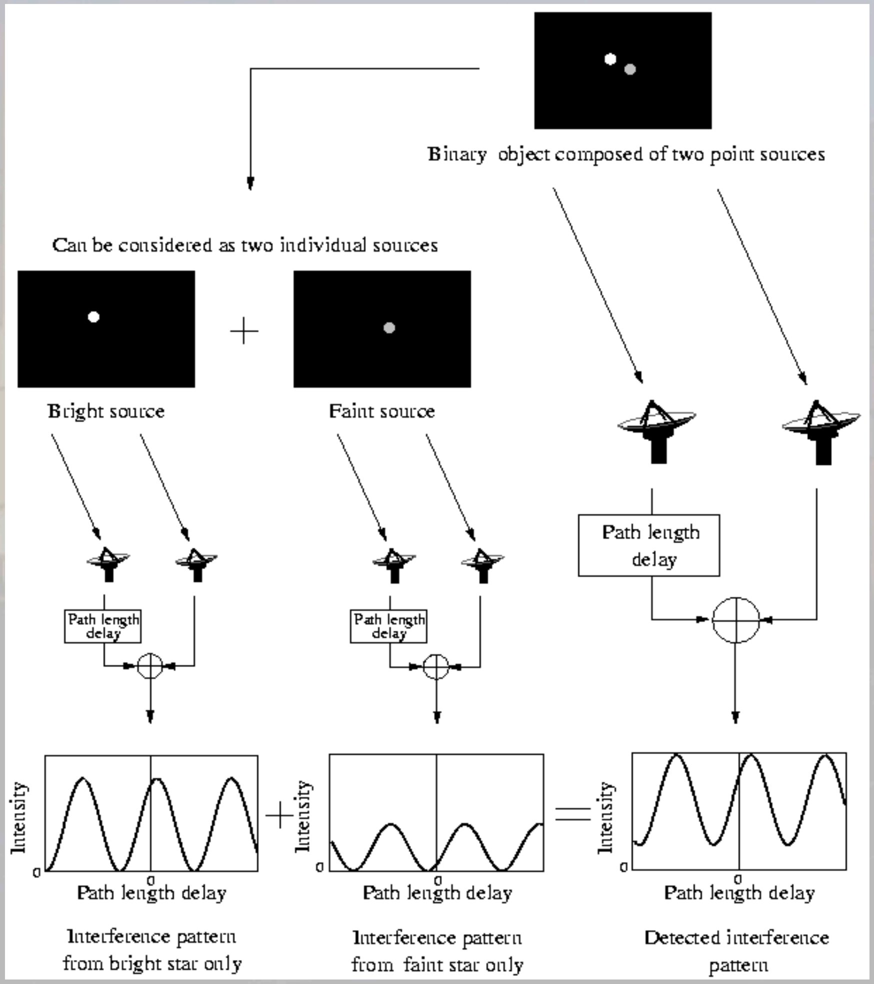

- The observed fringe pattern from a distributed source is just the intensity superposition of these individual fringe pattern.
- This relies upon the individual elements of the source being "spatially incoherent".

Heuristic operation of an interferometer

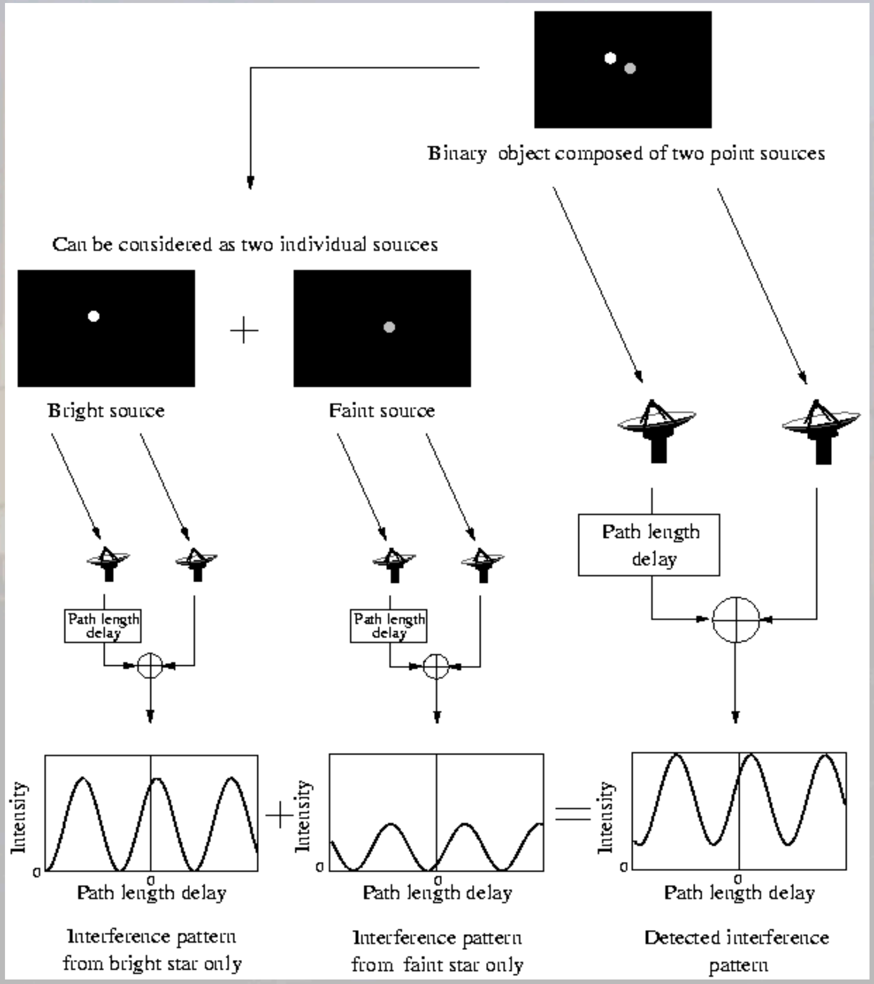

- The resulting fringe pattern has a modulation depth that is reduced with respect to that from each source individually.
- The positions of the sources are encoded (in a scrambled manner) in the resulting fringe phase.

Image deconvolution

Recall: $I(\vec{k}) = I_s + \underbrace{\cos(\vec{k}\vec{B}) \cdot Re|V|}_{\text{symmetric contrast}} + \underbrace{\sin(\vec{k}\vec{B})\, Im|V|}_{\text{anti-symmetric contrast}}$

For a given Baseline $\binom{u}{v}$ we can „mesure" $Re|V|$ and $Im|V|$.

$\Rightarrow$ Varying the Baseline $\longrightarrow V[u,v]$

· Since $V = \int A(\vec{k}_s) \cdot e^{-i\vec{k}_s\vec{B}}\, dk_s = \int A(\vec{k}_s) \cdot e^{-i\vec{k}_s \cdot \left[\begin{smallmatrix} u \\ v \end{smallmatrix}\right]} dk_s$

$= \hat{A}(u,v)$

we can redetermine the „shape" of the source by inverse fourier transform:

$$\underline{\underline{A(k_x,k_y)}} = \hat{V}(k_x,k_y) = \underline{\underline{\frac{1}{2\pi}\int V(u,v)\, e^{i\vec{k}\vec{B}}\, du\, dv}}$$

Extension to polychromatic light

- We can integrate the previous result over a range of wavelengths:
  - E.g for a uniform bandpass of $\lambda_0 \pm \Delta\lambda/2$ (i.e. $\nu_0 \pm \Delta\nu/2$) we obtain:

$$P \propto \int_{\lambda_0-\Delta\lambda/2}^{\lambda_0+\Delta\lambda/2} [2 + 2\cos(kD)]\, d\lambda$$

$$= \int_{\lambda_0-\Delta\lambda/2}^{\lambda_0+\Delta\lambda/2} 2\,[1 + \cos(2\pi D/\lambda)]\, d\lambda$$

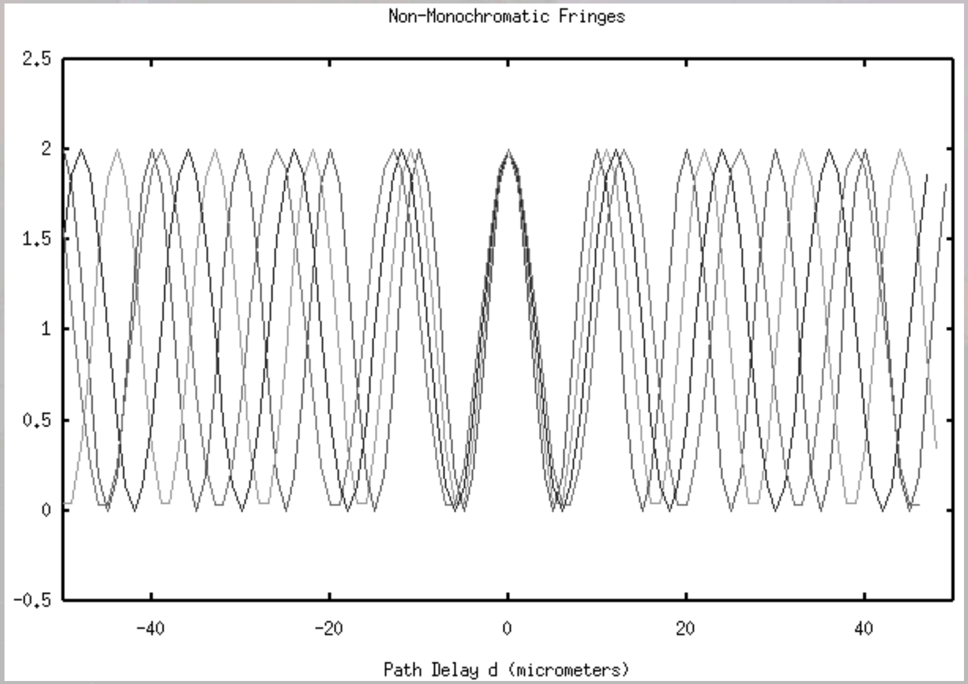

Extension to polychromatic light

- We can integrate the previous result over a range of wavelengths:
  - E.g for a uniform bandpass of $\lambda_0 \pm \Delta\lambda/2$ (i.e. $\nu_0 \pm \Delta\nu/2$) we obtain:

$$P \propto \int_{\lambda_0-\Delta\lambda/2}^{\lambda_0+\Delta\lambda/2} [2 + 2\cos(kD)]\, d\lambda$$

$$= \int_{\lambda_0-\Delta\lambda/2}^{\lambda_0+\Delta\lambda/2} 2\,[1 + \cos(2\pi D/\lambda)]\, d\lambda$$

$$= \Delta\lambda \left[1 + \frac{\sin \pi D \Delta\lambda / \lambda^2{}_0}{\pi D \Delta\lambda / \lambda^2{}_0} \cos k_0 D \right]$$

$$= \Delta\lambda \left[1 + \frac{\sin \pi D / \Lambda_{coh}}{\pi D / \Lambda_{coh}} \cos k_0 D \right]$$

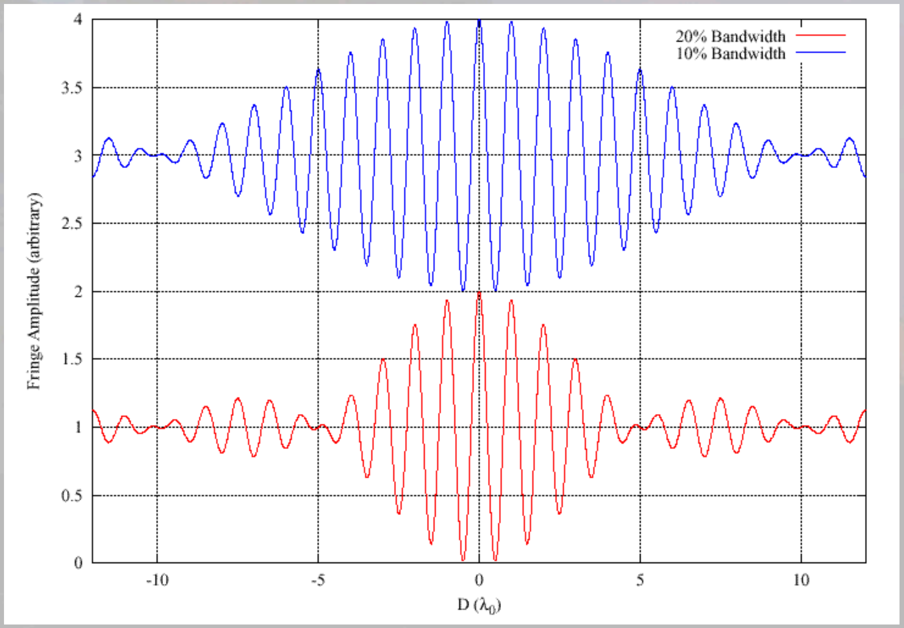

So, the fringes are modulated with an envelope with a characteristic width equal to the coherence length, $\Lambda_{coh} = \lambda^2_0/\Delta\lambda$.

A reality check

- How is all this related to the VLTI?
- Telescopes sample the fields at r_1 and r_2.
- Optical train delivers the radiation to a laboratory.
- Delay lines assure that we measure when $t_1=t_2$.
- The instruments mix the beams and detect the fringes.

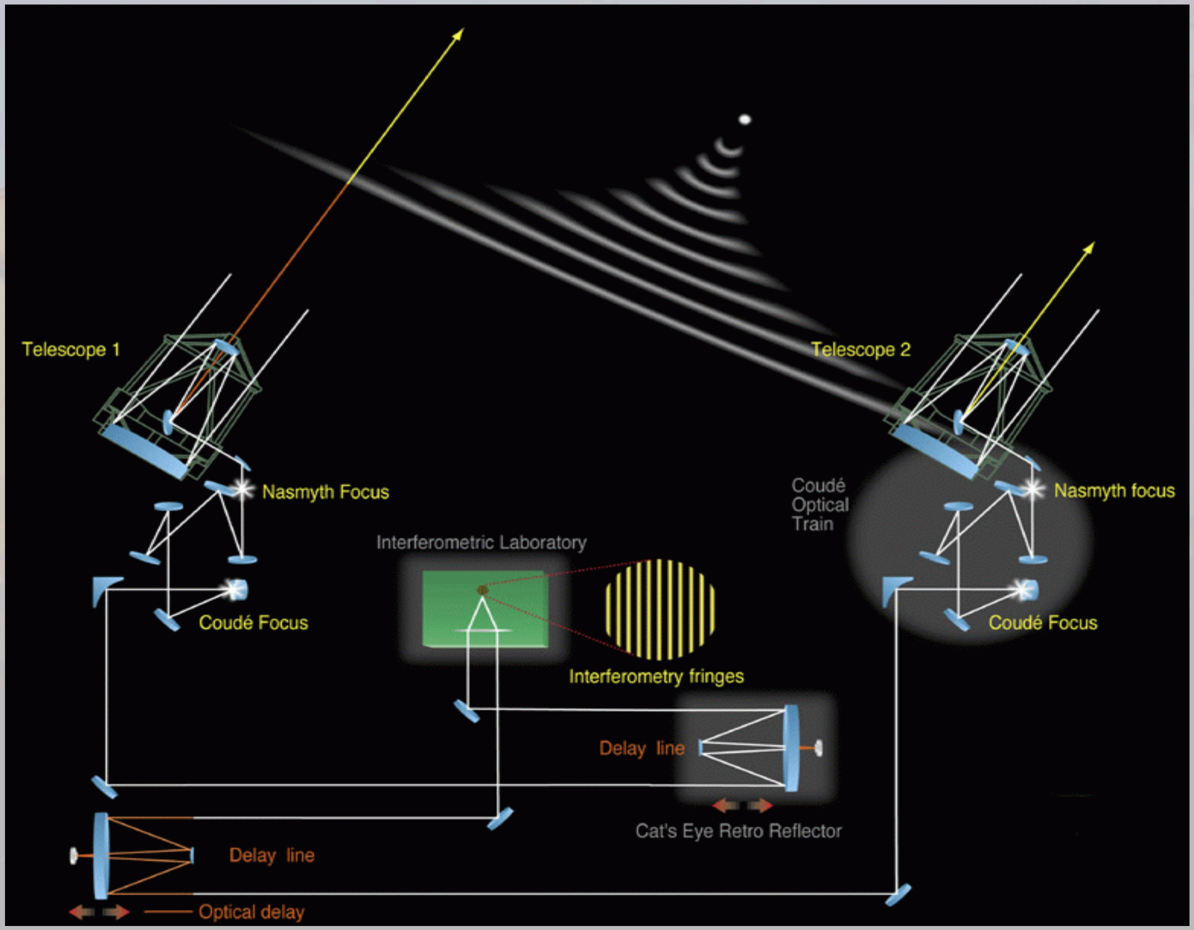

Simple 1-d sources (i)

$$V(u) = \int I(l)\, e^{-i2\pi(ul)}\, dl \div \int I(l)\, dl$$

Point source of strength A_1 and located at angle l_1 relative to the optical axis.

$$V(u) = \int A_1 \delta(l-l_1)\, e^{-i2\pi(ul)}\, dl \div \int A_1 \delta(l-l_1) dl$$
$$= e^{-i2\pi(ul_1)}$$

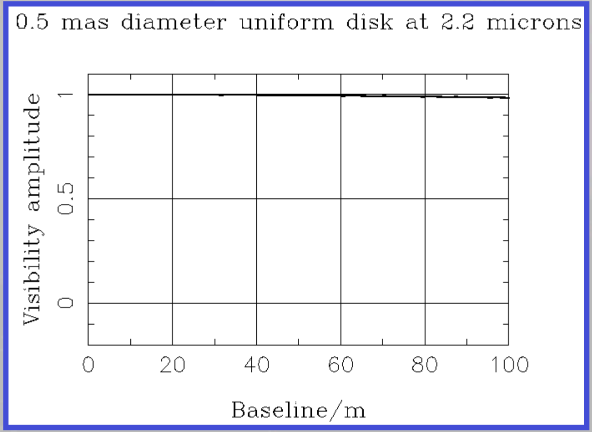

- The visibility amplitude is unity $\forall\, u$.
- The visibility phase varies linearly with u (= B/λ).
- Sources such as this are easy to observe (the fringes have high contrast), but are of little interest for imaging purposes.

Simple sources (ii)

A double source comprising point sources of strength A_1 and A_2 located at angles 0 and l_2 relative to the optical axis.

$$V(u) = \int [A_1\delta(l) + A_2\delta(l-l_2)]\, e^{-i2\pi(ul)}\, dl \div \int [A_1\delta(l) + A_2\delta(l-l_2)]\, dl$$
$$= [A_1 + A_2 e^{-i2\pi(ul_2)}] \div [A_1 + A_2]$$

- The visibility amplitude and phase oscillate as functions of u.

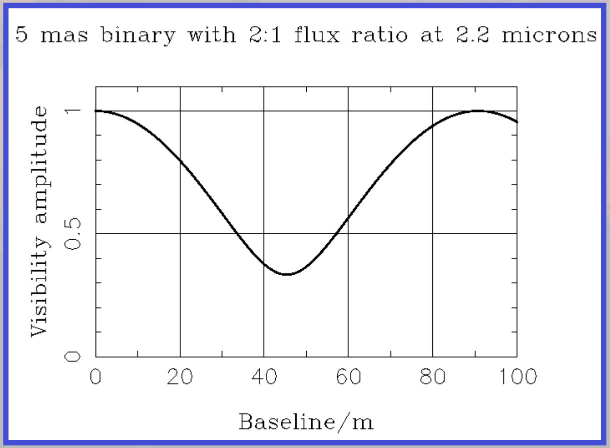

- To identify this as a binary, baselines from $0 \rightarrow \lambda/l_2$ are required.
- If the ratio of component fluxes is large the modulation of the visibility becomes increasingly difficult to measure.

Simple sources (iii)

A uniform on-axis disc source of diameter θ.

$$V(u_r) \propto \int^{\theta/2} \rho \, J_0(2\pi\rho u_r) \, d\rho$$
$$= 2J_1(\pi\theta u_r) \div (\pi\theta u_r)$$

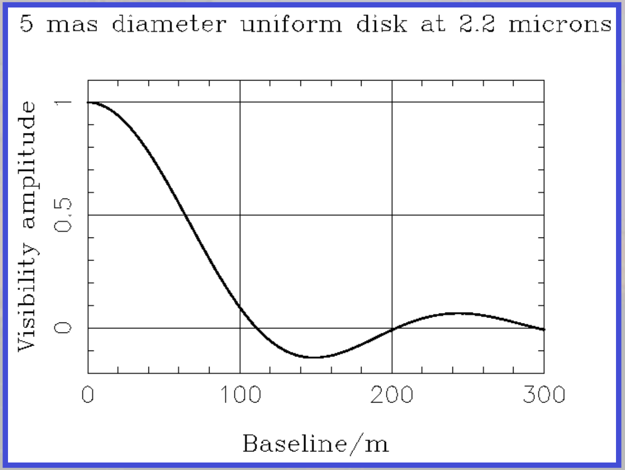

- The visibility amplitude falls rapidly as u_r increases.
- To identify this as a disc requires baselines from $0 \rightarrow \lambda/\theta$ at least.
- Information on scales smaller than the disc diameter correspond to values of u_r where V << 1, and is hence difficult to measure.

What can we learn from this?

- Distinguishing between different types of sources => measuring fringes for many different baseline lengths.
- The spatial properties of the image are encoded in the different changes in fringe contrast and phase seen as the baseline is altered.
- Point-like targets => fringes that have high contrast, and so are easy to measure.
- Resolved targets => fringes that are difficult to measure.

Understanding the expected values of V is key to designing a useful interferometer.

Image reconstruction

- We start with the fundamental relationship between the visibility function and the normalized sky brightness:

$$I_{\mathrm{norm}}(\mathrm{l}, \mathrm{m}) = \iint V(u, v)\, \mathrm{e}^{+\mathrm{i}2\pi(u\mathrm{l} + v\mathrm{m})}\, \mathrm{d}u\, \mathrm{d}v$$

- In practice what we measure is a sampled version of $V(u, v)$, so the image we have access to is to the so-called "dirty map":

$$I_{\mathrm{dirty}}(\mathrm{l}, \mathrm{m}) = \iint S(u, v)\, V(u, v)\, \mathrm{e}^{+\mathrm{i}2\pi(u\mathrm{l} + v\mathrm{m})}\, \mathrm{d}u\, \mathrm{d}v$$

$$= B_{\mathrm{dirty}}(\mathrm{l}, \mathrm{m}) * I_{\mathrm{norm}}(\mathrm{l}, \mathrm{m}) \;,$$

  where $B_{\mathrm{dirty}}(\mathrm{l},\mathrm{m})$ is the Fourier transform of the sampling distribution, or dirty-beam.

- The dirty-beam is the interferometer PSF. While it is generally far less attractive than an Airy pattern, it's shape is completely determined by the samples of the visibility function that are measured.

Deconvolution in interferometry

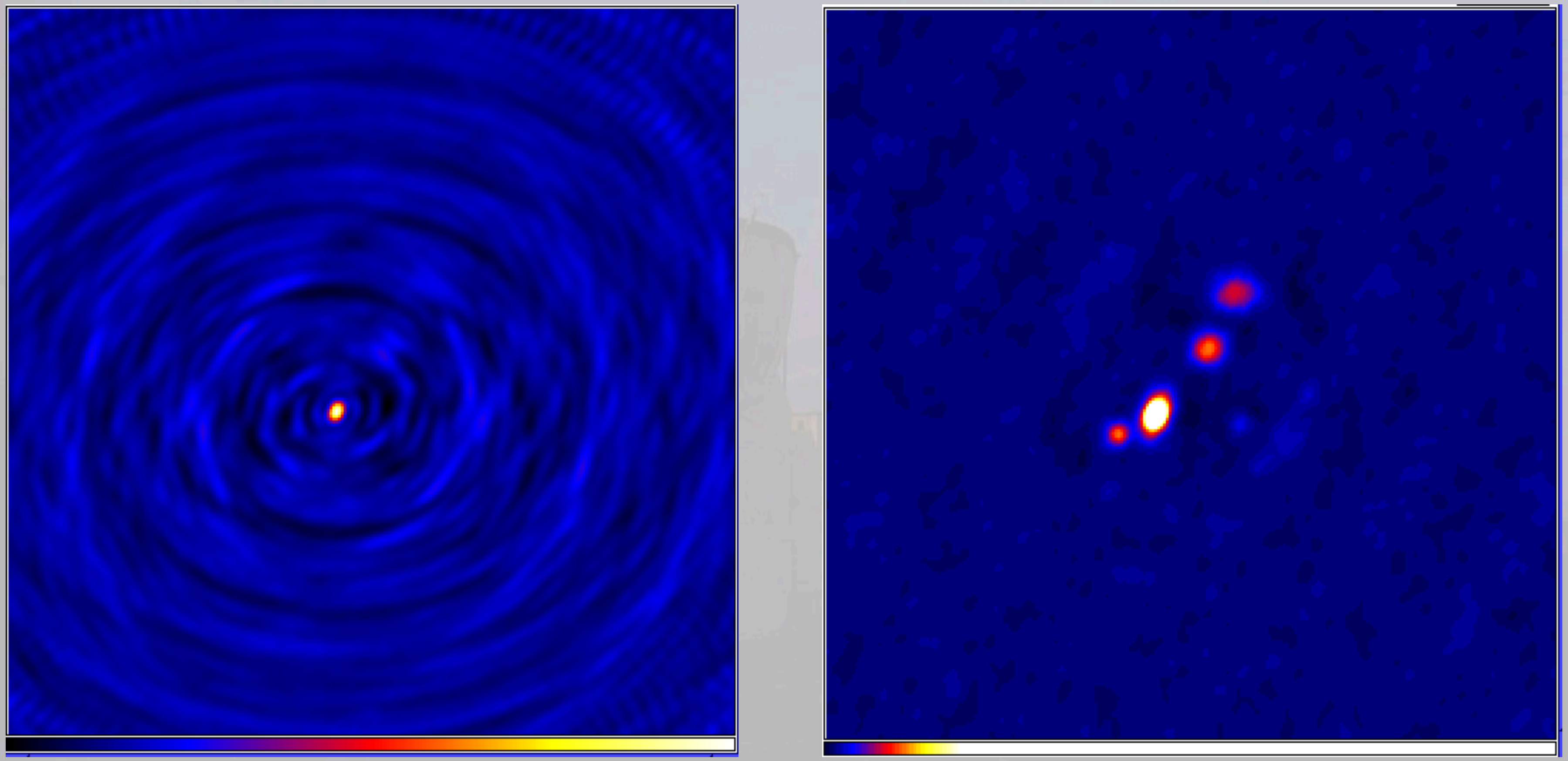

- Correcting an interferometric map for the Fourier plane sampling function is known as deconvolution (CLEAN, MEM, WIPE).

What is an appropriate UV-plane sampling?

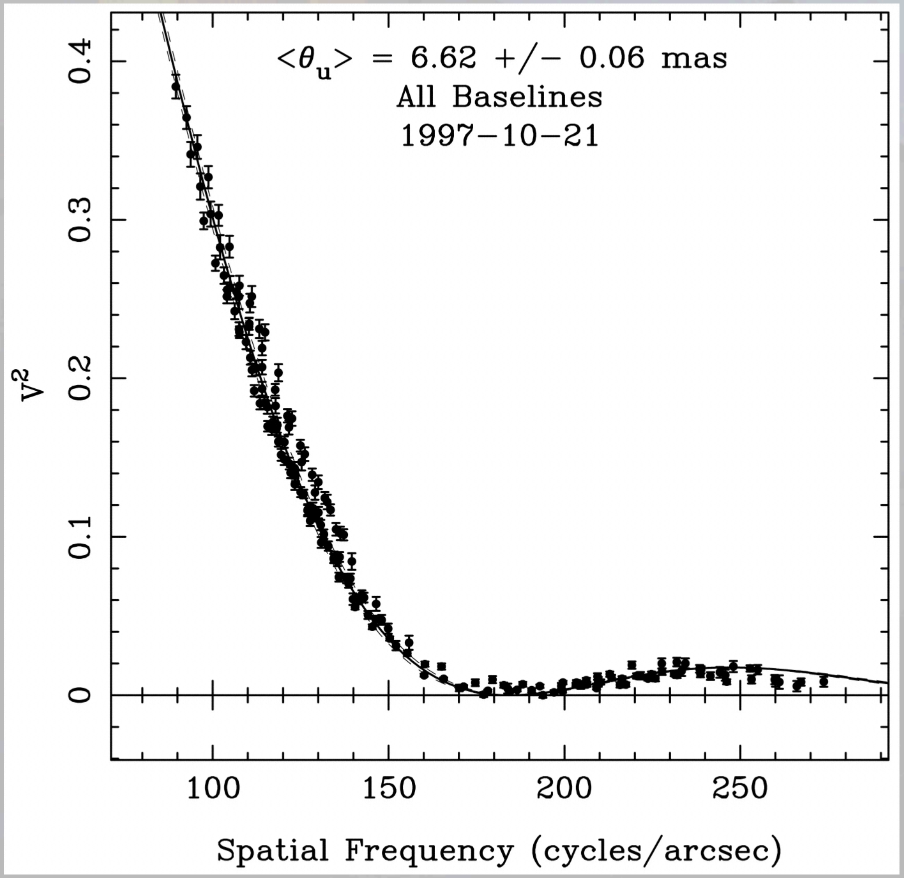

- Radius measurement with NPOI
- N telescopes >2
- accuracy on $V^2 > 1\%$
- impressive UV coverage
- use of spectral resolution to improve UV coverage

What is an appropriate UV-plane sampling?

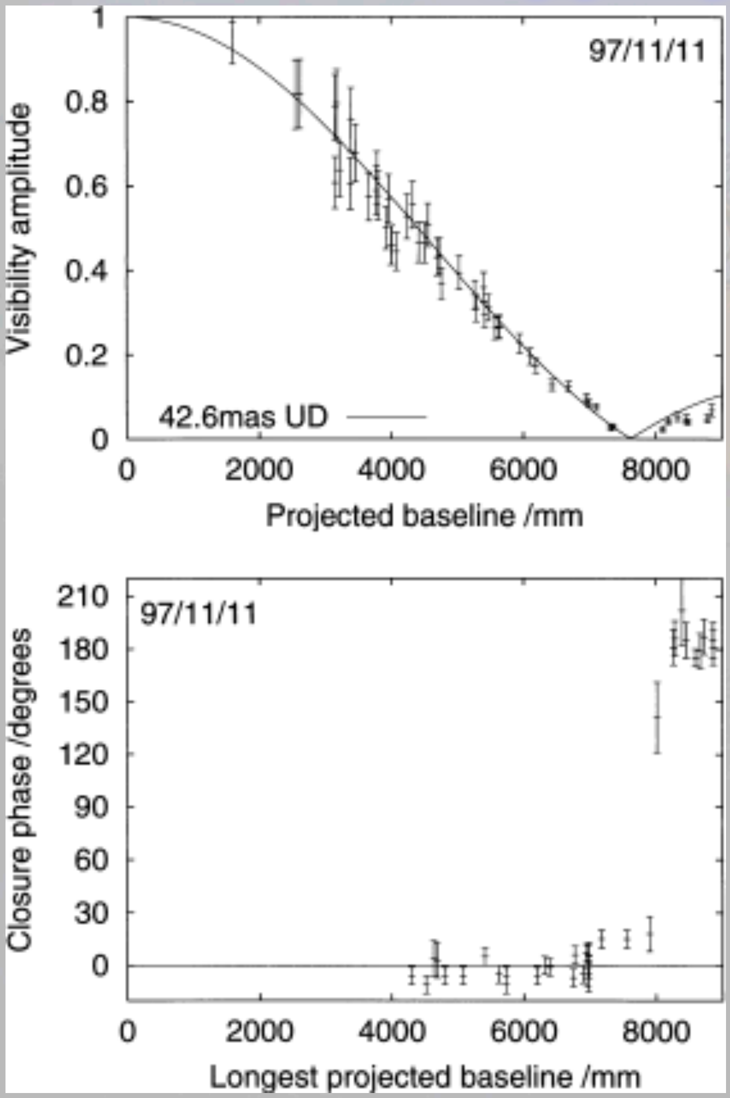

Radius measurement with COAST

- N telescopes = 3
- accuracy on $V^2 > 5\%$
- good UV coverage
- π transition in the closure phase is observed

What is an appropriate UV-plane sampling?

- Radius measurement with IOTA/ FLUOR
- N telescope = 2 (at that time)
- accuracy on $V^2 << 1\%$
- poor UV coverage but … a few points
- at the right place do the job

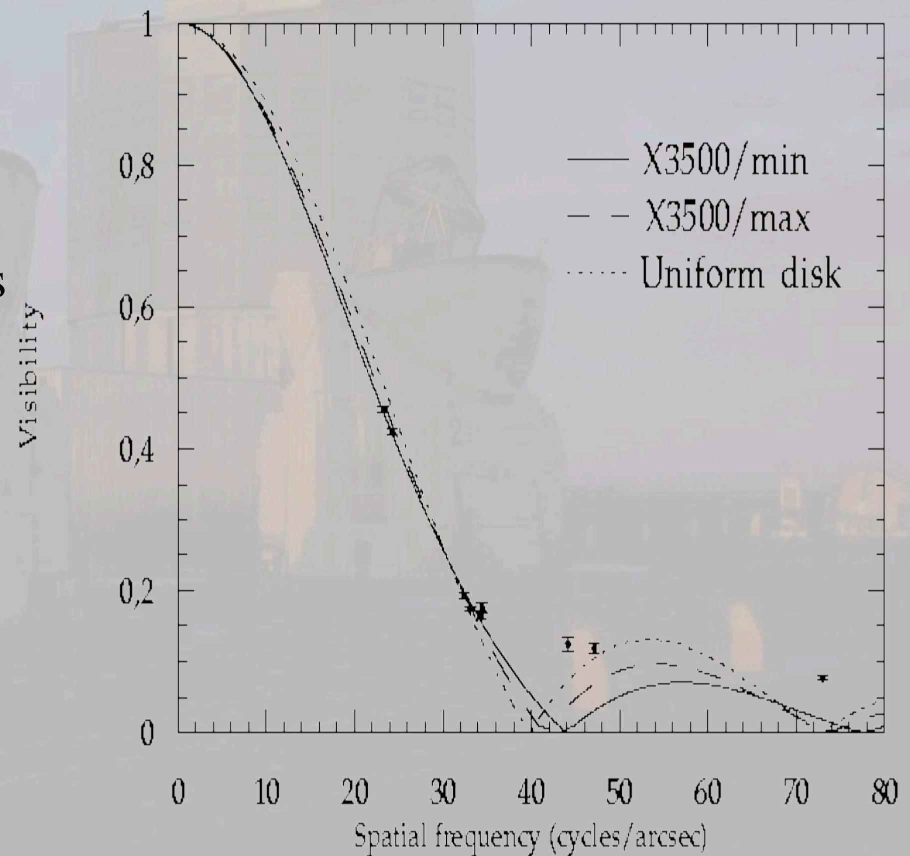

Interest to observe at mm wavelengths

visible

Star: 3000-100’000 K
Ionized gas: 10’000K

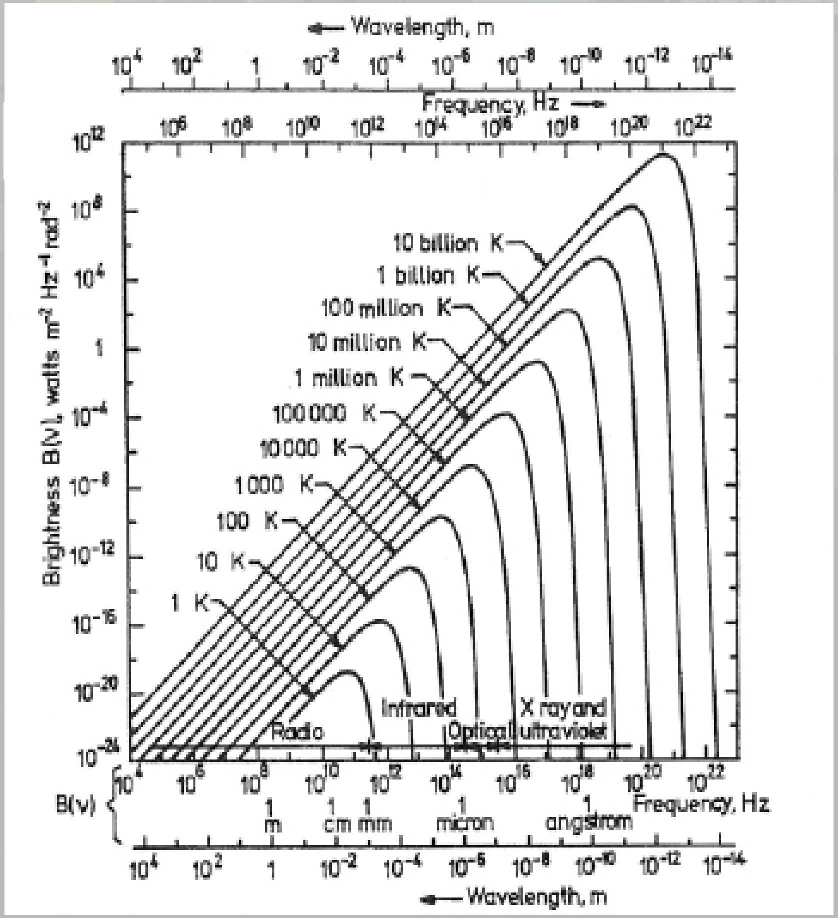

millimeter

Cold matter: 3-70 K
Dust and molecules

- Peak of black body emission:

  $\lambda = hc/3kT = 0.48/T$ cm
  → $T = 3$ K, $\lambda = 1$ mm
  $T = 10$ K, $\lambda = 0.3$ mm

- Peak of dust emission:

  $\lambda = hc/(3+\beta)kT = 0.3/T$ [cm]

- Typical energies involved in molecular transitions
- SED of galaxies
- SZ effect

Examples (1)

Black body emission:
cosmic microwave background radiation

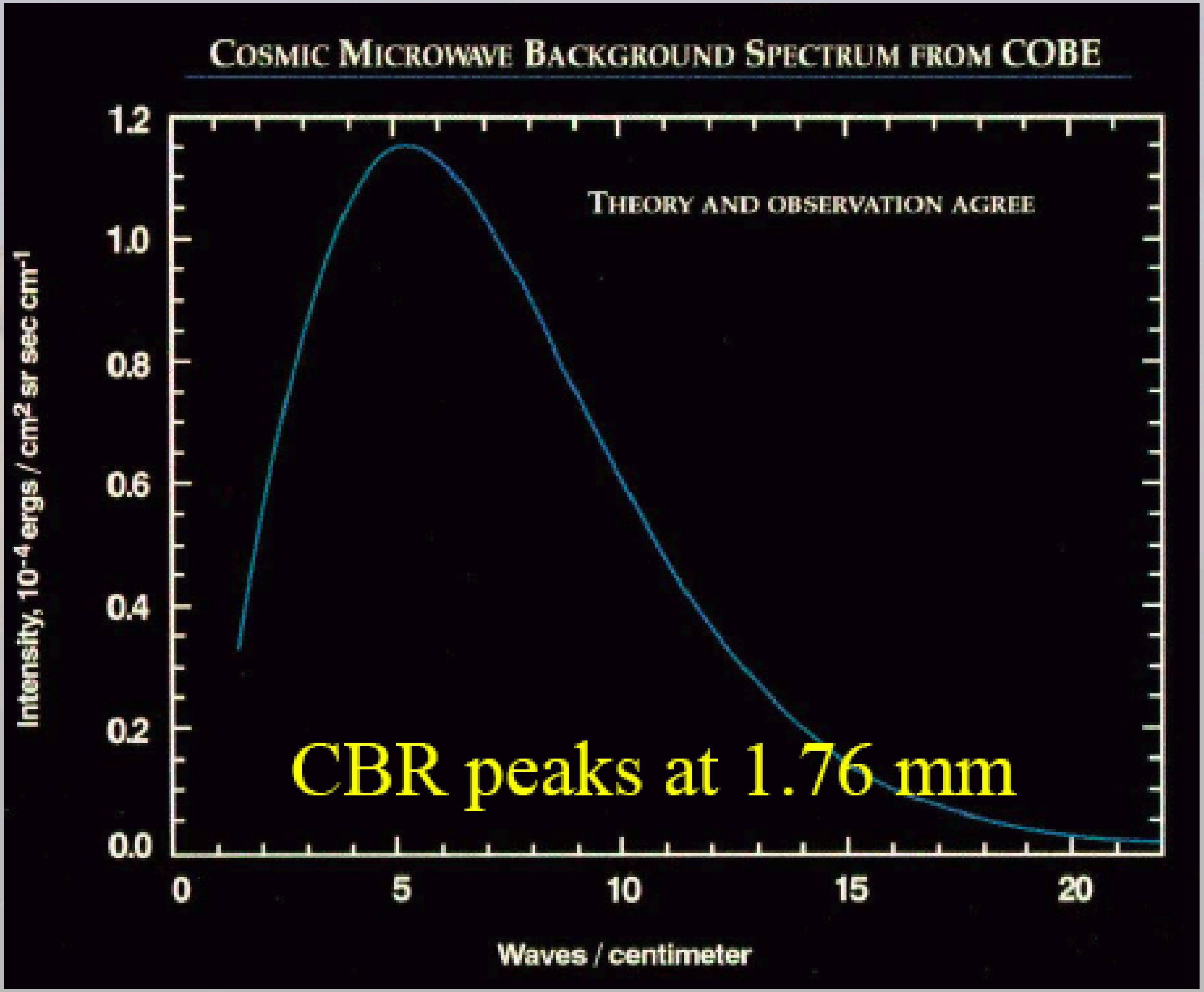

Examples (2)

Diffuse cloud properties:

$n = 10\text{-}10^3\ \mathrm{cm}^{-3}$

$T = 20\text{-}100$ K

$A_V < 1$

Dark cloud properties:

$n = 10^3\text{-}10^6\ \mathrm{cm}^{-3}$

$\underline{T = 8\text{-}15\ \mathrm{K}}$

$A_V > 1$

peak of dust emission
at 0.3 mm

Examples (3)

Typical energies involved in molecular transitions:

molecular low-energy rotational transitions lie at mm wavelengths

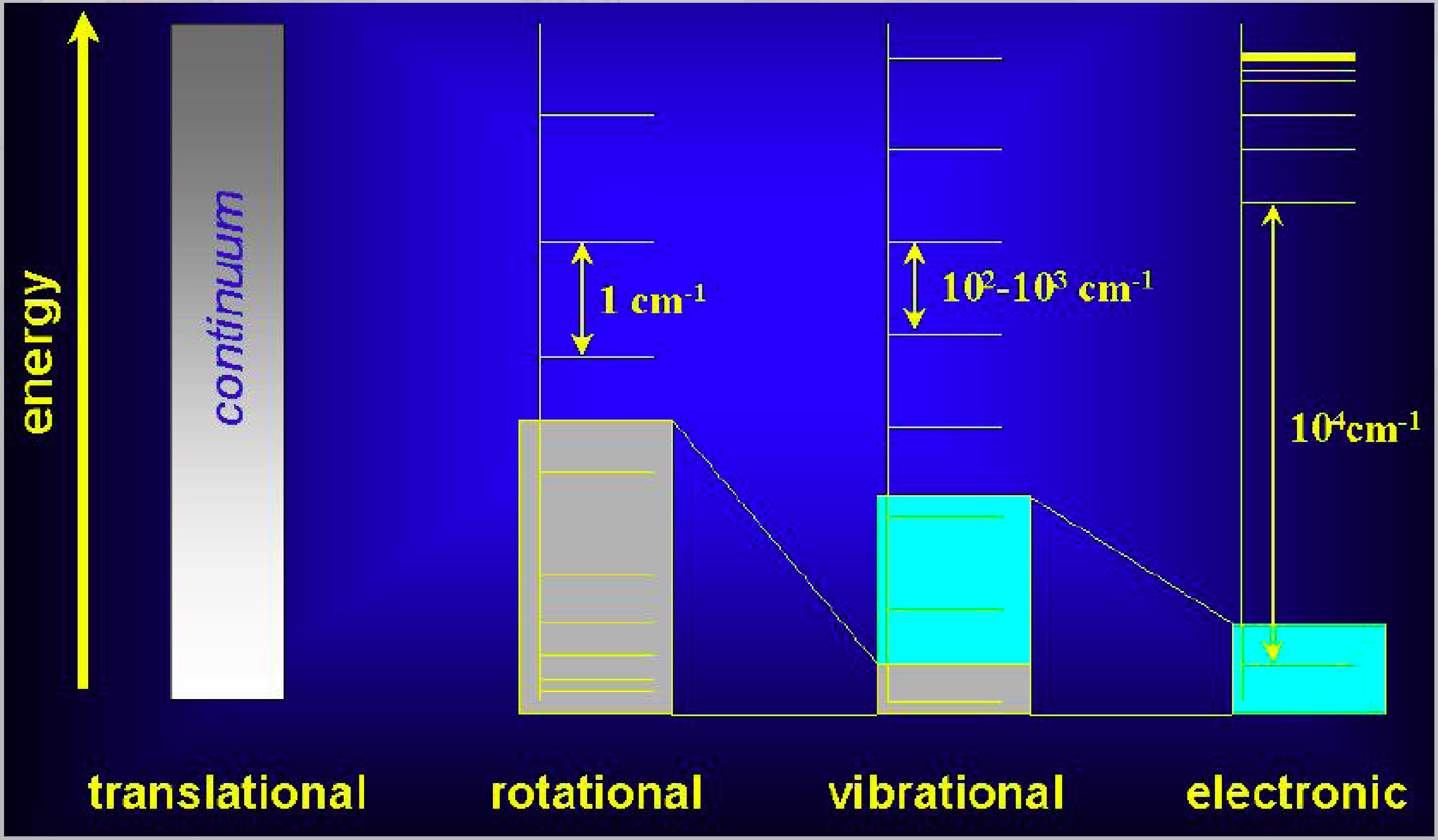

Examples (3)

Presently, more than 140 molecular species have been detected in the ISM:

Hydrogen Compounds

H_2	HD	H_3^+	H_2D^+		

Hydrogen and Carbon Compounds

CH	CH^+	C_2	CH_2	C_2H	*C_3
CH_3	C_2H_2	C_3H(lin)	c-C_3H	*CH_4	C_4
c-C_3H_2	H_2CCC(lin)	C_4H	*C_5	*C_2H_4	C_5H
H_2C_4(lin)	*HC_4H	CH_3C_2H	C_6H	*HC_6H	H_2C_6
*C_7H	CH_3C_4H	C_8H	*C_6H_6		

Hydrogen, Carbon (possibly) and Oxygen Compounds

OH	CO	CO^+	H_2O	HCO	HCO^+
HOC^+	C_2O	CO_2	H_3O^+	$HOCO^+$	H_2CO
C_3O	CH_2CO	HCOOH	H_2COH^+	CH_3OH	CH_2CHO
CH_2CHOH	CH_2CHCHO	HC_2CHO	C_5O	CH_3CHO	c-C_2H_4O
CH_3OCHO	CH_2OHCHO	CH_3COOH	CH_3OCH_3	CH_3CH_2OH	CH_3CH_2CHO
$(CH_3)_2CO$	$HOCH_2CH_2OH$	$C_2H_5OCH_3$	$(CH_2OH)_2CO$	CH_3CONH_2	

Hydrogen, Carbon (possibly) and Nitrogen Compounds

NH	CN	N_2	NH_2	HCN	HNC
N_2H^+	NH_3	$HCNH^+$	H_2CN	HCCN	C_3N
CH_2CN	CH_2NH	HC_2CN	HC_2NC	NH_2CN	C_3NH
CH_3CN	CH_3NC	HC_3NH^+	*HC_4N	C_5N	CH_3NH_2
CH_2CHCN	HC_5N	CH_3C_3N	CH_3CH_2CN	HC_7N	CH_3C_5N?
HC_9N	$HC_{11}N$				

Examples (4)

M82 in the radio, mm, sub-mm and FIR

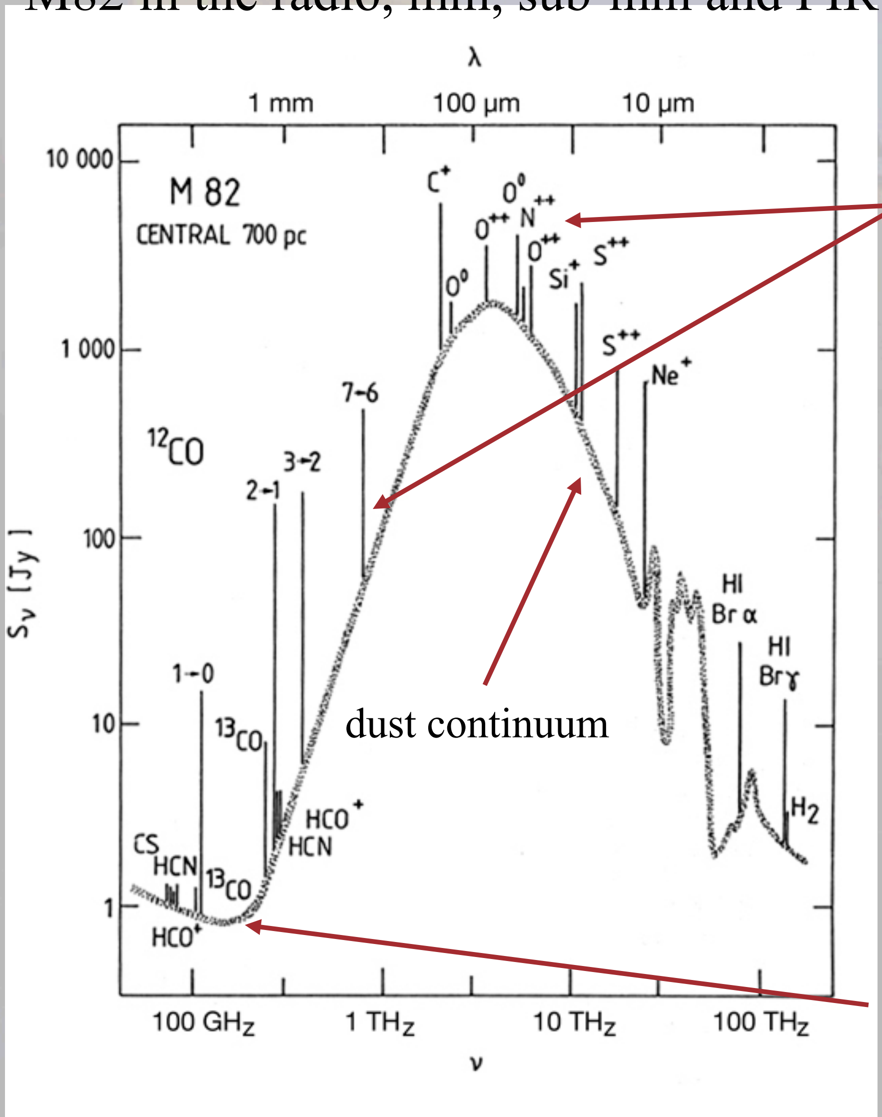

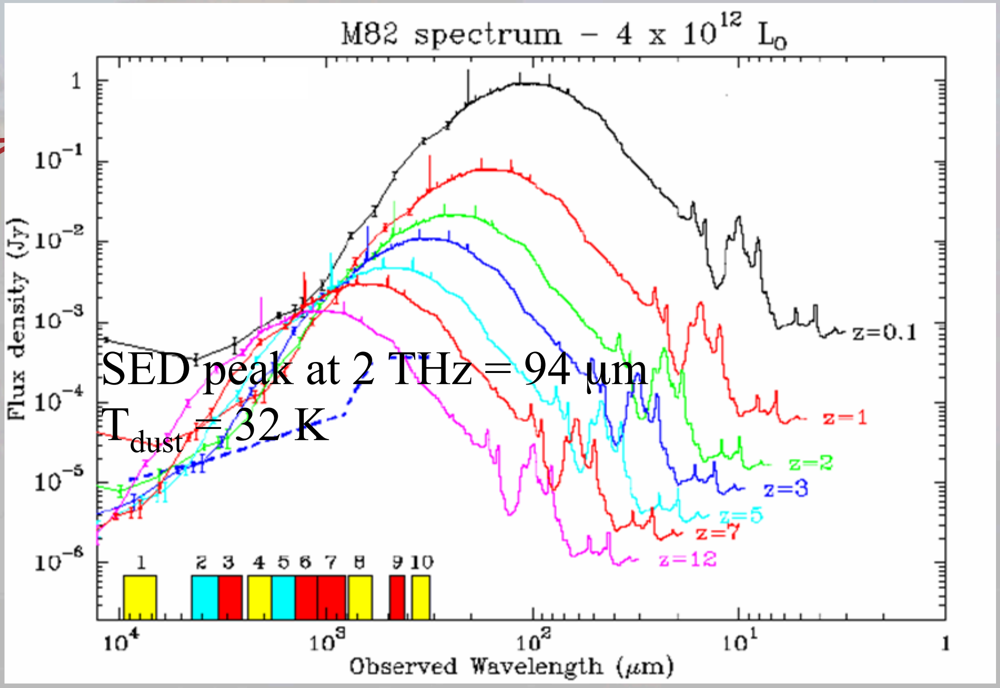

bremstrahlung+synchrotron continuum

Observing techniques

Receivers in use at FIR and mm wavelengths:

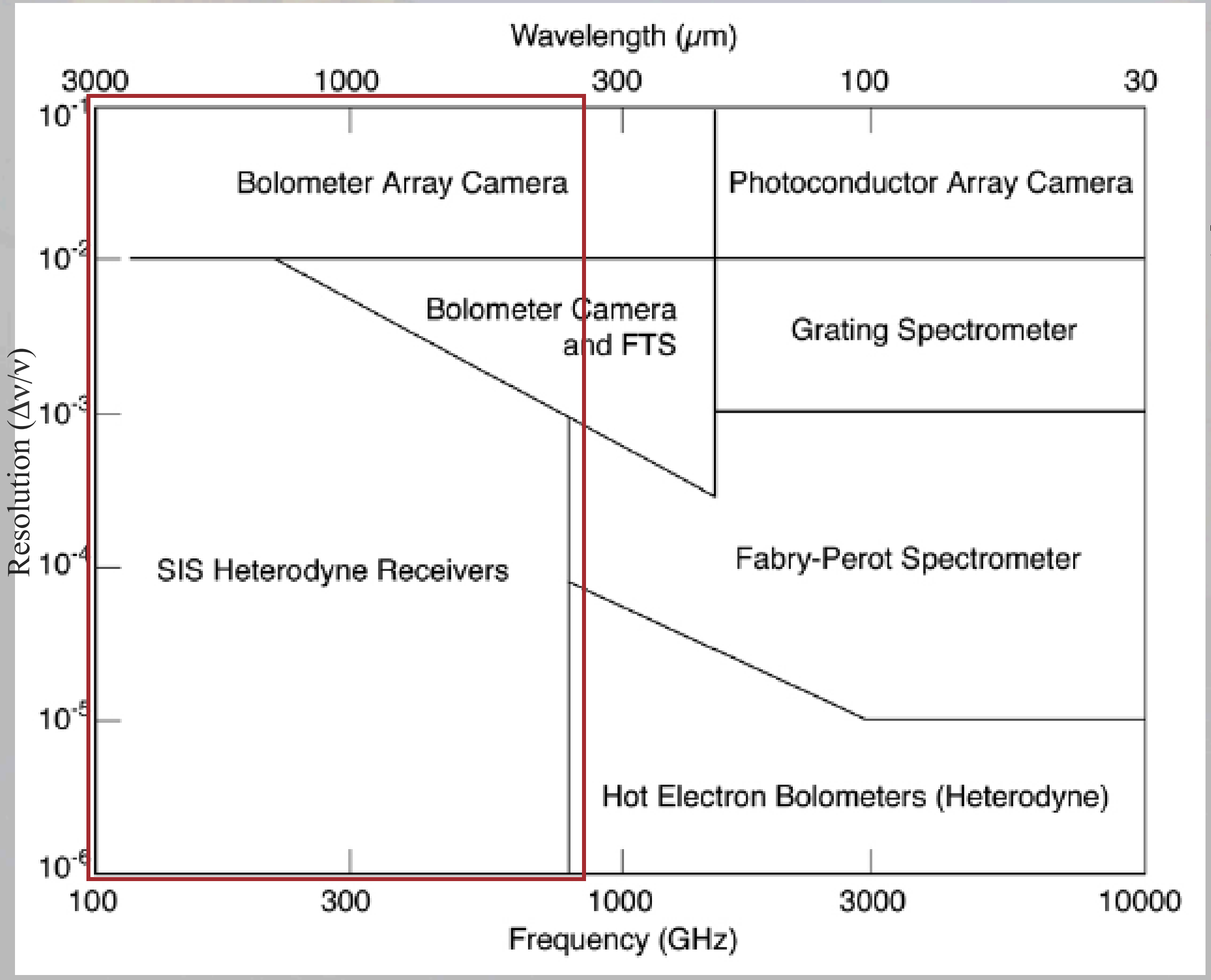

<u>Bolometers</u>:
used for imaging

<u>Heterodyne receivers</u>:
used for spectroscopy

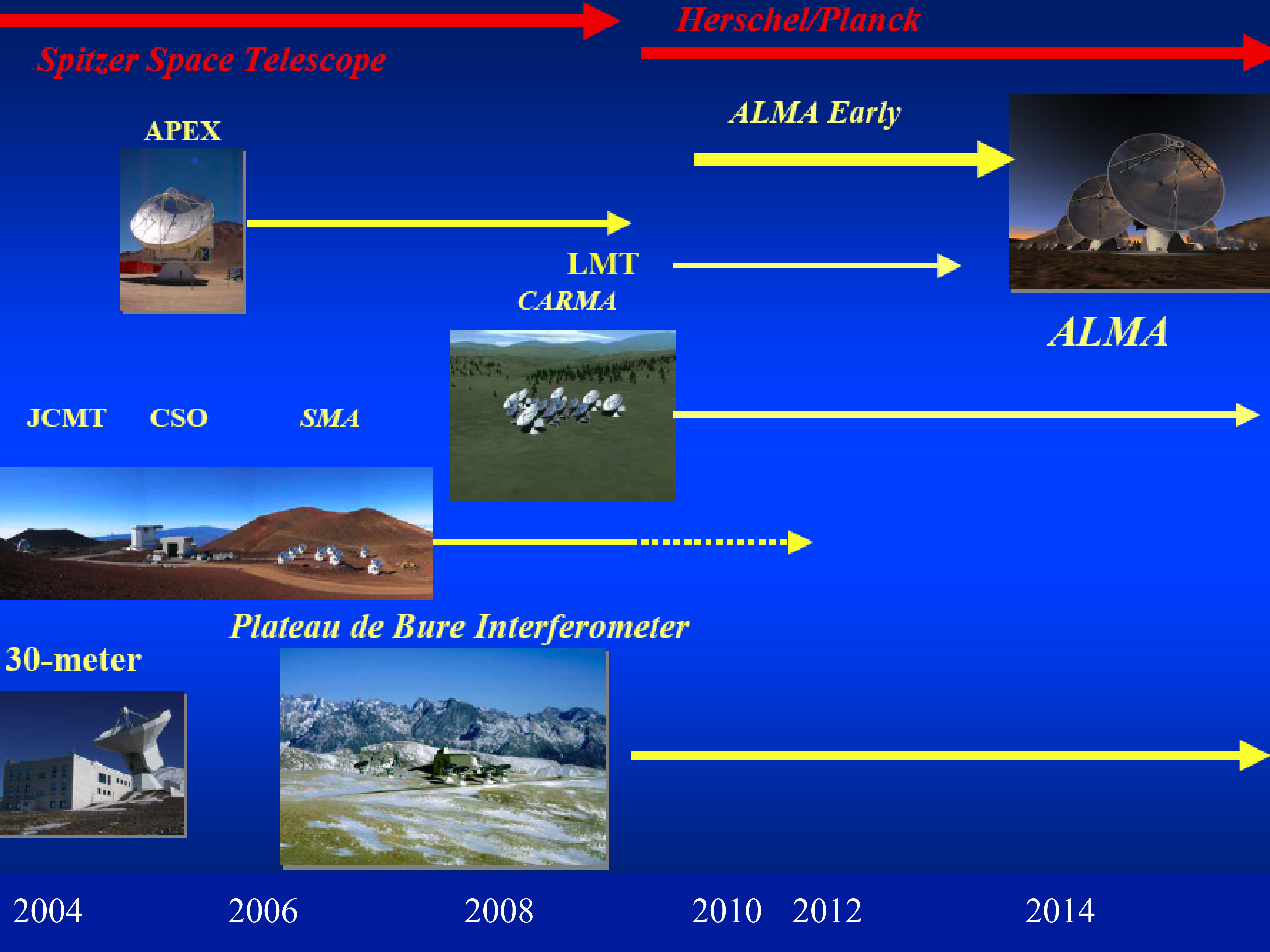
Spitzer Space Telescope
Herschel/Planck
APEX
ALMA Early
LMT
CARMA
ALMA
JCMT
CSO
SMA
Plateau de Bure Interferometer
30-meter
2004
2006
2008
2010
2012
2014

50 ANTENNES DE 12 m DE DIAMETRE VONT COMPOSER UN SEUL INSTRUMENT

RESEAU COMPACT:
4 ANTENNES DE 12 m + 12 DE 7 m
→ utile pour couvrir les short-spacings

SURFACE COLLECTRICE: ~ 5600 m^2
plus la surface collectrice est grande,
plus la sensibilité est élevée

SPECIFICATIONS DE CHAQUE ANTENNE:

- 25 μm rms sur la surface
- 2” de pointage absolu
- 0.6” de suivi des cibles

ANTENNES: 3 PROTOTYPES

JAPON	MITSUBISHI	4 x 12 m + 12 x 7 m
AMERIQUE DU NORD	VERTEX	25 x 12 m (→ 32)
EUROPE	ALCATEL	25 x 12 m (→ 32)

ALMA TEST FACILITY (SOCORRO, USA)